

Threitol-Strapped Manganese Porphyrins as Enantioselective Epoxidation Catalysts of Unfunctionalized Olefins

James P. Collman,^{*,1a} Virgil J. Lee,^{1a} Cynthia J. Kellen-Yuen,^{1a} Xumu Zhang,^{1a} James A. Ibers,^{1b} and John I. Brauman^{1a}

Contribution from the Departments of Chemistry, Stanford University, Stanford, California 94305, and Northwestern University, Evanston, Illinois 60208

Received June 29, 1994[⊗]

Abstract: Nine members of a family of new chiral porphyrins have been prepared from reactions between ditosylthreitol derivatives and 5,10,15,20-tetrakis(2-hydroxyphenyl)porphyrin. The assignment of the resultant isomers has been made from their ¹H NMR spectra and on the basis of an absolute configuration determination from the crystal structure of **4**. The chiral frameworks of these systems are easily varied by condensing different aldehydes and ketones with the 2,3-diol of the threitol unit. The manganese derivatives of six of these systems were studied as asymmetric catalysts in the epoxidation of unfunctionalized olefins. Up to 88% ee is obtained in the epoxidation of 1,2-dihydronaphthalene with one of these derivatives, **9**, when a bulky imidazole ligand is used to block the unhindered face of the porphyrin catalyst.

Introduction

The development of asymmetric catalysts that mediate the stereoselective formation of carbon–oxygen bonds is an important goal in the synthesis of optically active organic compounds. Effective chiral catalysts have been developed for asymmetric reactions such as the epoxidation of allylic alcohols² and the hydrogenation of functionalized ketone derivatives.³ Those catalysts must coordinate to the functionalized substrate to achieve high optical yields. The stereoselective formation of carbon–oxygen bonds from unfunctionalized substrates presents a greater challenge, because the catalysts for such systems rely solely on nonbonding interactions to achieve asymmetric induction. While recent progress has been reported in the enantioselective *cis*-dihydroxylation of simple olefins,⁴ most of the work performed on asymmetric carbon–oxygen bond-forming reactions has focused on the enantioselective epoxidation of unfunctionalized olefins.^{5,6}

Chiral manganese salen complexes currently are the most effective asymmetric catalysts for unfunctionalized olefins.⁵ Enantiomeric excesses (ee's) of greater than 90% have been reported in the epoxidation of *cis*-disubstituted olefins when NaOCl (bleach) was employed as the oxidant,^{5f,h} although lower optical yields are usually obtained with other olefin types. The

facile synthesis and ease of modifying these Schiff-base ligands has led to an optimization of the catalyst structure resulting in the preparation of more than 120 different chiral metallosalen derivatives.⁷ The major limitation of these systems is that metallosalens become inactive under the oxidation conditions and generally give less than 40 catalyst turnovers.^{5d}

Several manganese and iron derivatives of chiral porphyrins have also been examined as catalysts for the asymmetric epoxidation of unfunctionalized olefins.⁶ These porphyrin catalysts generally give lower enantiomeric excesses and are more difficult to synthesize than the corresponding chiral salen systems. However, metalloporphyrins generally exhibit greater catalytic stability than metallosalens in oxygenation reactions. For example, chiral metalloporphyrin catalysts have generated up to 2800 turnovers in asymmetric epoxidation.^{6c}

Two crucial factors govern the effectiveness of these chiral metalloporphyrin catalysts. First, to achieve substantial asym-

[⊗] Abstract published in *Advance ACS Abstracts*, December 1, 1994.

(1) (a) Stanford University. (b) Northwestern University.

(2) (a) Katsuki, T.; Sharpless, K. B. *J. Am. Chem. Soc.* **1980**, *102*, 5974–5976. (b) Gao, Y.; Hanson, R. M.; Klunder, J. M.; Ko, S. Y.; Masamune, H.; Sharpless, K. B. *J. Am. Chem. Soc.* **1987**, *109*, 5765–5780. (c) For a recent review, see: Johnson, R. A.; Sharpless, K. B. In *Comprehensive Organic Synthesis*; Trost, B. M., Fleming, I., Eds.; Pergamon: New York, 1991; Vol. 7, pp 389–436.

(3) (a) Takaya, H.; Ohta, T.; Sayo, N.; Kumobayashi, H.; Akutagawa, S.; Inoue, S.; Kasahara, I.; Noyori, R. *J. Am. Chem. Soc.* **1987**, *109*, 1596–1597. (b) Hayashi, T.; Kawamura, N.; Ito, Y. *J. Am. Chem. Soc.* **1987**, *109*, 7876–7878. (c) Koenig, K. E. In *Asymmetric Synthesis*; Morrison, J. D., Ed.; Academic: New York, 1985; Vol. 5, p 71.

(4) (a) Jacobsen, E. N.; Markó, I. E.; Mungall, W. S.; Schröder, G. W.; Sharpless, K. B. *J. Am. Chem. Soc.* **1988**, *110*, 1968–1970. (b) Wai, J. S. M.; Markó, I. E.; Svendsen, J. S.; Finn, M. G.; Jacobsen, E. N.; Sharpless, K. B. *J. Am. Chem. Soc.* **1989**, *111*, 1123–1125. (c) Sharpless, K. B.; Amberg, W.; Beller, M.; Chen, H.; Hartung, J.; Kawanami, Y.; Lübben, D.; Manoury, E.; Ogino, Y.; Shibata, T.; Ukita, T. *J. Org. Chem.* **1991**, *56*, 4585–4588. (d) Sharpless, K. B.; Amberg, W.; Bennani, Y. L.; Crispino, G. A.; Hartung, J.; Jeong, K.-S.; Kwong, H.-L.; Morikawa, K.; Wang, Z.-M.; Xu, D.; Zhang, X.-L. *J. Org. Chem.* **1992**, *57*, 2768–2771.

(5) (a) Zhang, W.; Loebach, J. L.; Wilson, S. R.; Jacobsen, E. N. *J. Am. Chem. Soc.* **1990**, *112*, 2801–2803. (b) Irie, R.; Noda, K.; Ito, Y.; Matsumoto, N.; Katsuki, T. *Tetrahedron Lett.* **1990**, *31*, 7345–7348. (c) Irie, R.; Noda, K.; Ito, Y.; Matsumoto, N.; Katsuki, T. *Tetrahedron Asym.* **1991**, *2*, 481–494. (d) Zhang, W.; Jacobsen, E. N. *J. Org. Chem.* **1991**, *56*, 2296–2298. (e) Jacobsen, E. N.; Zhang, W.; Güler, M. *J. Am. Chem. Soc.* **1991**, *113*, 6703–6704. (f) Jacobsen, E. N.; Zhang, W.; Muci, A. R.; Ecker, J. R.; Ding, L. *J. Am. Chem. Soc.* **1991**, *113*, 7063–7064. (g) Lee, N. H.; Jacobsen, E. N. *Tetrahedron Lett.* **1991**, *32*, 6533–6536. (h) Lee, N. H.; Muci, A. R.; Jacobsen, E. N. *Tetrahedron Lett.* **1991**, *32*, 5055–5058. (i) Irie, R.; Noda, K.; Ito, Y.; Katsuki, T. *Tetrahedron Lett.* **1991**, *32*, 1055–1058. (j) O'Connor, K. J.; Wey, S.-J.; Burrows, C. J. *Tetrahedron Lett.* **1992**, *33*, 1001–1004. (k) Hosoya, N.; Irie, R.; Katsuki, T. *Synlett* **1993**, 261–263.

(6) (a) Groves, J. T.; Meyers, R. S. *J. Am. Chem. Soc.* **1983**, *105*, 5791–5796. (b) Mansuy, D.; Battioni, P.; Renaud, J.-P.; Guerin, P. *J. Chem. Soc., Chem. Commun.* **1985**, 155–156. (c) O'Malley, S.; Kodadek, T. *J. Am. Chem. Soc.* **1989**, *111*, 9116–9117. (d) Groves, J. T.; Viski, P. *J. Org. Chem.* **1990**, *55*, 3628–3634. (e) Halterman, R. L.; Jan, S.-T. *J. Org. Chem.* **1991**, *56*, 5253–5254. (f) Naruta, Y.; Tani, F.; Ishihara, N.; Maruyama, K. *J. Am. Chem. Soc.* **1991**, *113*, 6865–6872. (g) Licocchia, S.; Paci, M.; Tagliatesta, P.; Paolesse, R.; Antonaroli, S.; Boschi, T. *Magn. Reson. Chem.* **1991**, *29*, 1084–1091. (h) Maillard, P.; Guerquin-Kern, J. L.; Momenteau, M. *Tetrahedron Lett.* **1991**, *32*, 4901–4904. (i) Konishi, K.; Oda, K.-I.; Nishida, K.; Aida, T.; Inoue, S. *J. Am. Chem. Soc.* **1992**, *114*, 1313–1317. (j) Collman, J. P.; Zhang, X.; Lee, V. J.; Brauman, J. I. *J. Chem. Soc., Chem. Commun.* **1992**, 1647–1649. (k) Naruta, Y.; Ishihara, N.; Tani, F.; Haruyama, K. *Bull. Chem. Soc. Jpn.* **1993**, *66*, 158–168. (l) For a recent review of asymmetric epoxidations, see: Collman, J. P.; Zhang, X.; Lee, V. J.; Uffelman, E.; Brauman, J. I. *Science*, **1993**, *261*, 1404–1411.

(7) Jacobsen, E. N., private communication.

metric induction, the chiral unit must interact effectively with the olefin during the oxidation process. Since the active oxidant forms at the metal center,⁸ the chiral moieties should be close to the center of the macrocycle where the oxidation occurs. Second, the chiral units cannot be too close to the active site because manganese and iron porphyrins can even oxidize unactivated alkanes,⁹ making the chiral units themselves potential substrates in metalloporphyrin-catalyzed oxidations utilizing these metals. Thus, close proximity of the chiral substituents to the metal might induce intramolecular oxidation of these substituents that would alter or destroy the catalyst.

Herein we report the preparation of nine members of a family of easily modified chiral porphyrins. The chiral frameworks in these systems are constructed from threitol straps that are easily varied by changing the protecting group used at the 2,3-diol positions of the threitol unit. This systematic study has produced a chiral manganese porphyrin, **9** (Scheme 2), that is one of the most effective asymmetric epoxidation catalysts for unfunctionalized olefins. This account describes the preparation and characterization of these chiral porphyrins. The catalytic activity of the manganese derivatives of six of these systems is also reported. A portion of this work was communicated earlier.¹⁰

Results

As an extension of our earlier work on shape-selective epoxidation with mono-faced porphyrin systems,¹¹ we sought to develop a mono-faced porphyrin that would effectively catalyze enantioselective epoxidations. The advantages of a mono-faced porphyrin that functions as an asymmetric catalyst are that it should be easier to synthesize and it should require less precious chiral material than the corresponding bis-faced system. Such a single-faced system relies upon bulky ligands to block the unhindered face of the porphyrin, forcing the reaction to occur on the substituted face and yielding the desired selectivity.^{6i,11} Our strategy has been to prepare an easily modifiable, mono-faced system in which chiral units bridge the adjacent phenyl groups of a tetraarylporphyrin, while the 2,3-positions could be derivitized as ether, ester, acetal, or ketal groups. Thus, modification of the chiral environment over the porphyrin would be achieved by varying the size and shape of the protecting groups used in the tartrate strap.

Many of the chiral porphyrins described in the literature have been prepared from reactions between chiral acid chlorides and 5,10,15,20-tetrakis(2-aminophenyl)porphine (TAPP).^{6a,b,d,g,j,k} This is an effective approach because it yields stable, amide-linked systems and because the atropisomers of TAPP can be isolated

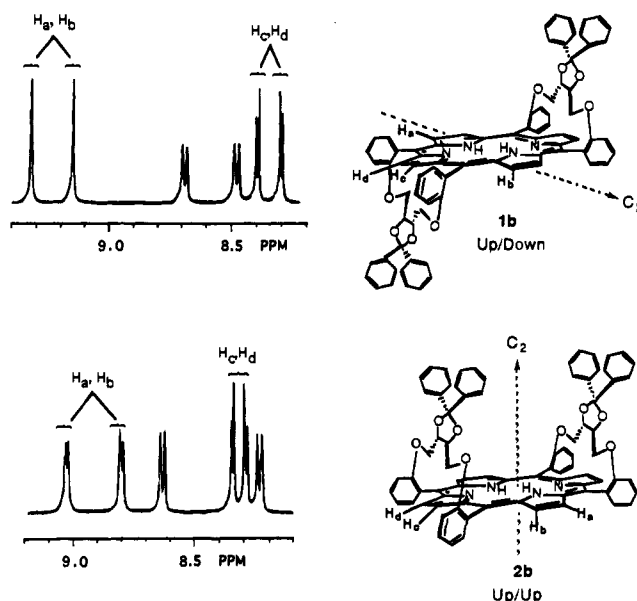


Figure 1. ¹H NMR spectra showing peaks corresponding to the β -pyrrolic protons on the Up/Down and the Up/Up isomers of the unbridged, threitol-strapped free base porphyrins **1b** and **2b**, respectively.

and are stable to rotation at room temperature.¹² Unfortunately, our attempts at preparing bis-strapped systems from reactions between tartaric acid chloride derivatives and TAPP isomers led only to intractable materials.¹³

Momenteau developed an alternative strategy for the preparation of strapped-porphyrin systems from 5,10,15,20-tetrakis(2-hydroxyphenyl)porphine (**10**).¹⁴ In this approach, **10** is condensed with α,ω -dibromoalkanes under basic conditions to form a bis-ether strapped system. This reaction is performed with an atropisomer mixture of **10** because its atropisomers interconvert at room temperature.¹⁵ Although this interconversion limits the control over the orientation of the straps, this strategy simplifies the synthesis because the individual atropisomers do not have to be isolated.

Synthesis. Two different classes of chiral porphyrins—bridged and unbridged—have been synthesized from reactions between **10** and ditosylthreitol derivatives. The unbridged porphyrins have been prepared by condensing a ketal-protected ditosylthreitol (**11**) with **10** (Scheme 1) to give two types of strapped porphyrins, **1** and **2**. These products differ by the relative orientation of the threitol straps; **1** has a simple strap on each face of the porphyrin (Up/Down) and **2** has both straps on the same face (Up/Up). A third possible isomer¹⁴ in which the straps bridge the diagonal positions of the macrocycle is not formed, presumably because the threitol derivatives are too short to span these positions across the porphyrin.

The strapped porphyrins **1** and **2** are easily separated by chromatography; structural assignments are based on differences in their ¹H NMR spectra. While both isomers have C_2 symmetry, their principal rotation axes are in different locations, resulting in differences in the splitting patterns of their β -pyrrolic hydrogen peaks (Figure 1). The C_2 axis of **1** is in the porphyrin plane, bisecting the pyrrole rings situated between the chiral straps. The adjacent hydrogen atoms at these β -pyrrolic positions are equivalent and thus do not split one another,

(8) For a recent review of metalloporphyrin catalyzed oxidations, see: Gunter, M. J.; Turner, P. *Coord. Chem. Rev.* **1991**, *108*, 115–161.

(9) For hydroxylations catalyzed by iron porphyrins, see: (a) Groves, J. T.; Nemo, T. E.; Myers, R. S. *J. Am. Chem. Soc.* **1979**, *101*, 1032–1033. (b) Groves, J. T.; Nemo, T. E. *J. Am. Chem. Soc.* **1983**, *105*, 5786–5791. For hydroxylations catalyzed by manganese porphyrins, see: (c) Hill, C. L.; Scharidt, B. C. *J. Am. Chem. Soc.* **1980**, *102*, 6374–6375. (d) Groves, J. T.; Kruper, W. J.; Haushalter, R. C. *J. Am. Chem. Soc.* **1980**, *102*, 6375–6377.

(10) (a) Collman, J. P.; Lee, V. J.; Zhang, X.; Ibers, J. A.; Brauman, J. I. *J. Am. Chem. Soc.* **1993**, *115*, 3834–3835. (b) Collman, J. P.; Lee, V. J.; Zhang, X.; Kellen-Yuen, C. J. U.S. Patent Series 08/045,497 **1993**.

(11) (a) Collman, J. P.; Zhang, X.; Hembre, R. T.; Brauman, J. I. *J. Am. Chem. Soc.* **1990**, *112*, 5356–5357. (b) Collman, J. P.; Zhang, X.; Lee, V. J.; Hembre, R. T.; Brauman, J. I. in *Homogeneous Transition Metal Catalyzed Reactions*; Moser, W. R., Slocum, D. W., Eds.; ACS Advances in Chemistry Series 23; American Chemical Society: Washington, DC, 1992; pp 152–162.

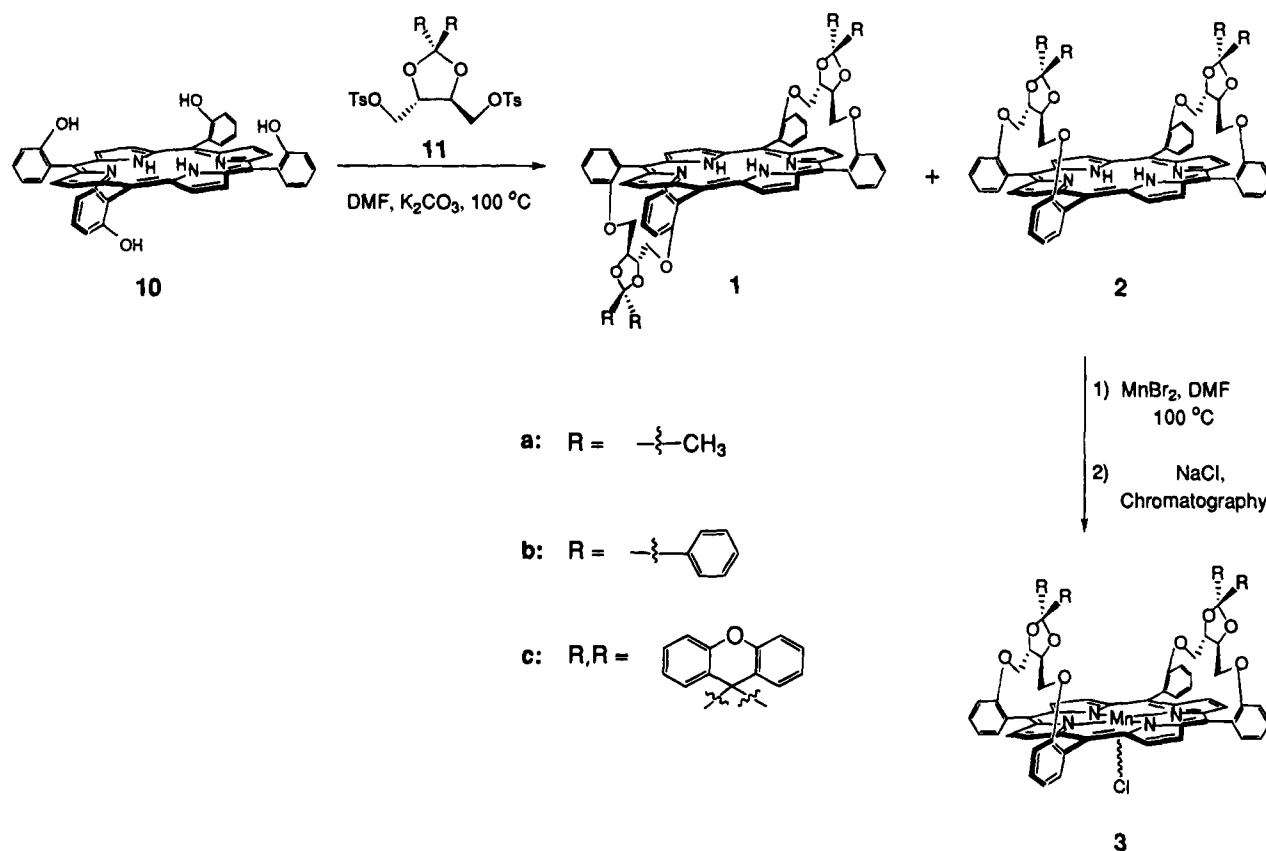
(12) Collman, J. P.; Gagné, R. R.; Reed, C. A.; Halbert, T. R.; Lang, R.; Robinson, W. T. *J. Am. Chem. Soc.* **1975**, *97*, 1427–1439.

(13) Zhang, X.; Lee, V. J., unpublished results.

(14) Momenteau, M.; Mispelter, J.; Loock, B.; Bisagni, E. *J. Chem. Soc., Perkin Trans. 1* **1983**, 189–196.

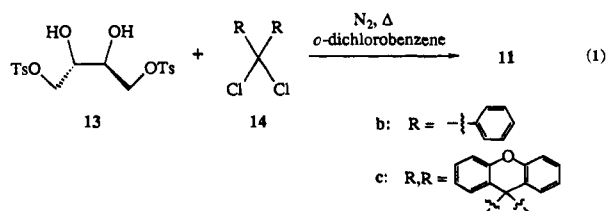
(15) Gottweld, L. K.; Ullman, E. F. *Tetrahedron Lett.* **1969**, 3071–3074.

Scheme 1. Synthesis of Unbridged, Threitol-Strapped Porphyrins

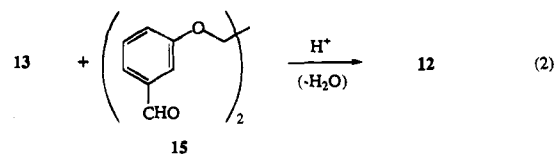


yielding two singlets in the ^1H NMR spectrum of **1**. In addition, two sets of doublets are observed for the inequivalent β -pyrrolic hydrogen atoms on the pyrrole rings under the straps. The C_2 axis of **2** is perpendicular to the porphyrin plane and intersects the center of the macrocycle (Figure 1). Thus the adjacent hydrogen atoms at each of the adjacent β -pyrrolic positions are inequivalent and four set of doublets are observed in the ^1H NMR spectrum of **2**.

Derivatives of **1** and **2** have been prepared from three different ditsylthreitol compounds, **11a–c**. This material is commercially available when R = methyl (**11a**). The direct formation of **11b** and **11c** from (*S,S*)-1,4-ditsylthreitol (**13**) and the corresponding ketone was unsuccessful in our hands under standard ketal-forming conditions. However, reactions between **13** and the corresponding geminal dichloride (**14**) do afford these ketals (eq 1).¹⁶ The combined yields of **1** and **2** range from 37% (R = methyl) to 52% (R = phenyl). In each case, the Up/Up isomer (**2**) is the major product.



The bridged chiral porphyrins (Scheme 2) are modified versions of **2** in which the threitol straps are connected by a bridge that spans the center of the macrocycle. These bridged systems are prepared from the condensation of **10** with **12**. The tetratosylated, bis-threitol derivative **12** is prepared from the condensation of **13** with **15** (eq 2). The bridge forces the threitol



straps to form on the same face of the porphyrin. However, the inequivalent substituents H and R on the acetal carbon atoms of the threitol strap permit the formation of three stereoisomers (Scheme 2)—**4** (In/In), **5** (In/Out), and **6** (Out/Out)—which can be separated by chromatography. These isomers differ by the stereochemistry at the acetal carbon atoms. Isomers **4** and **6** have C_2 symmetry and are distinguishable from **5** (which has C_1 symmetry) by ^1H NMR spectroscopy. The assignment of the C_2 isomers is based on an X-ray crystal structure of **4** (see below). The combined yield of these isomers is 44%, with **5** as the major product (23%), followed by **6** (16%), and then **4** (4.6%).

The manganese(III) chloride porphyrin derivatives **3a–c** and **7–9** were prepared by metalating the corresponding free base porphyrins with manganese(II) bromide in air, followed by exchange of the counterion in the reaction workup procedure.¹⁷ The manganese derivatives of the Up/Down isomers (**1a–c**) were not prepared because similar chiral porphyrin isomers have been shown to be ineffective epoxidation catalysts.^{6a}

X-ray Structure of 4. Crystals of **4**· CD_2Cl_2 suitable for X-ray analysis were obtained by slow evaporation of a CD_2Cl_2 solution of the free base porphyrin **4** over a 1-week period. Data were collected on a CAD4 diffractometer. The structure was solved by direct methods¹⁸ and refined by full-matrix least-

(17) Powell, M. F.; Pai, E. F.; Bruice, T. C. *J. Am. Chem. Soc.* **1984**, *106*, 3277–3285.

(18) Shelldrick, G. M. SHELXTL PC Version 4.1 An integrated system for solving, refining, and displaying crystal structures from diffraction data. Siemens Analytical X-Ray Instruments, Inc.: Madison, WI.

(16) Hobbs, C.; Knowles, W. S. *J. Org. Chem.* **1981**, *46*, 4422–4427.

Scheme 2. Synthesis of Bridged, Threitol-Strapped Porphyrins

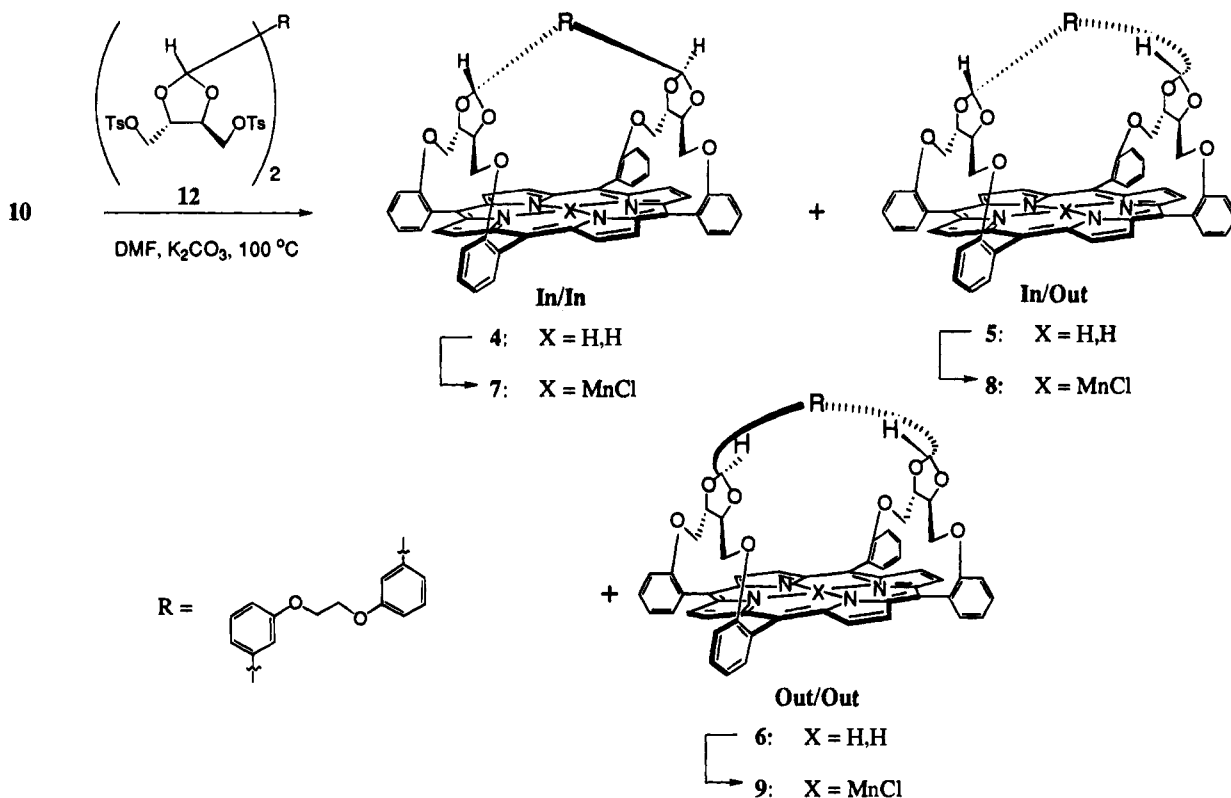


Table 1. Crystallographic Data for the In/In Isomer, 4

chemical formula	$\text{C}_{68}\text{H}_{52}\text{N}_4\text{O}_{10}\cdot 2\text{CD}_2\text{Cl}_2$
formula wt, amu	1259.1
a , Å	18.925(5)
c , Å	16.974(10)
V , Å ³	6079(2)
space group	$C_4^6 - I4_1$
Z	4
$\mu(\text{Mo K}\alpha)$, cm^{-1}	2.60
ρ_{calc} (g/cm^3)	1.375
T , K	115
$R(F_o)^a$ ($F_o^2 > 2\sigma(F_o^2)$)	0.068
$R_w(F_o^2)^b$ (all data)	0.131

^a $R_w(F_o) = \sum ||F_o| - |F_c|| / \sum |F_o|$. ^b $R_w(F_o^2) = \{\sum [w(F_o^2 - F_c^2)^2] / \sum w F_o^4\}^{1/2}$; $w^{-1} = \sigma^2(F_o^2) + (0.04 F_o^2)^2$; $w^{-1} = \sigma^2(F_o^2)$, $F_o^2 < 0$.

squares techniques.¹⁹ This material crystallizes in the polar space group $I4_1$ with four formula units in the cell, and as a result 4 has a crystallographically imposed C_2 axis, as deduced from the NMR spectroscopy. The effects of anomalous scattering, resulting from the fortuitous presence of the CD_2Cl_2 molecules in the cell, permitted the determination of the chirality of 4, which was that expected from the synthetic chemistry. Details concerning the data collection and refinement are given in Table 1. The R -indices are higher than normal owing to our inability to model satisfactorily the disorder that is apparent in one of the solvent molecules.

The labeling scheme and thermal ellipsoids are shown in Figure 2; a stereoview of 4 is displayed in Figure 3. The supplementary material contains Table S1 (crystal data and structure refinement), Table S2 (atomic coordinates and equivalent isotropic displacement parameters), Table S3 (bond lengths and angles), Table S4 (anisotropic displacement parameters), and Table S5 (hydrogen atom coordinates and isotropic displacement parameters). Within the porphyrin moiety the bond lengths and angles are normal. However, the porphyrin is distorted (Figure 3), probably as a result of the steric constraints

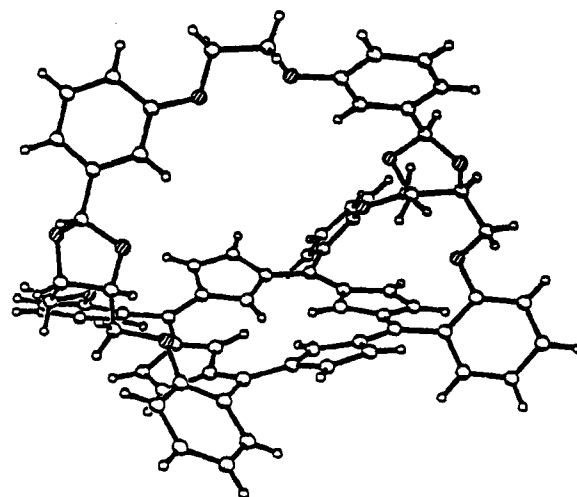


Figure 2. A drawing of the structure of 4, showing the labeling scheme and the 50% probability ellipsoids. Hydrogen atoms have been omitted. The molecule has a crystallographically imposed C_2 axis.

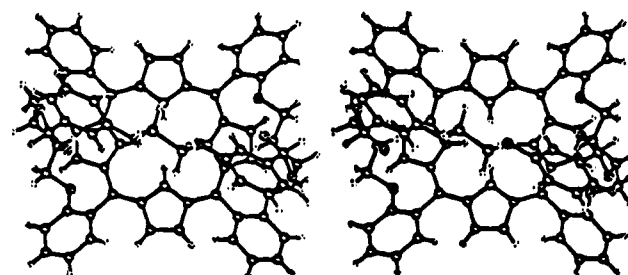


Figure 3. A stereoview of the structure of 4. The oxygen atoms are cross hatched while the hydrogen atoms are small. The half hydrogen atoms in the center of the porphyrin are shown.

of the threitol straps that bridge the adjacent *meso*-phenyl substituents. This distortion is manifested in several ways: (1) the average deviation of the N and C atoms from the 24-atom

Table 2. Asymmetric Epoxidation Catalyzed by **3b**^a

entry	olefin	yield, ^{b,c} %	ee, ^d %	optical rotation ^e
1	styrene	64	39	R(+)
2	4-nitrostyrene	61	15	R(+)
3	4-chlorostyrene	95	44	R(+)
4	4-phenylstyrene	73	33	R(+)
5	4-methylstyrene	63	42	R(+)
6	2-nitrostyrene	64	37	(-) ^f
7	<i>o</i> -methylstyrene	51	51	(-) ^f
8	2,3,4,5,6-pentafluorostyrene	94	26	R(+)
9	2-vinylnaphthalene	65	40	R(+)
10	<i>cis</i> - β -methylstyrene	76 ^g	59	1 <i>R</i> ,2 <i>S</i> (-)
11	dihydronaphthalene	87	38	1 <i>R</i> ,2 <i>S</i> (+)
12	<i>trans</i> - β -methylstyrene	39	17	1 <i>S</i> ,2 <i>s</i> (-)
13	2-methyl-1-phenylpropene	51	10	(+) ^f

^a Reactions were generally run for 1 h with 1.0 μ mol of **3b**, 100 μ mol of iodosylbenzene, 20 μ L of nonane or dodecane, and 1.00 mmol of olefin in 2 mL of dry CH₂Cl₂ under nitrogen. ^b Yields are based upon consumption of iodosylbenzene and were determined by GC analysis. ^c The yields of oxidized products in entries 1–11 are greater than 85% with the remainder of the product being the corresponding aldehydes or ketones. ^d Determined by Cyclodex-B chiral capillary column or by ¹H NMR spectroscopy in the presence of Eu(hfc)₃. ^e Assigned by comparison of polarimetry measurements with literature. ^f The absolute configuration was not determined. ^g 7.5% of *trans*- β -methylstyrene oxide is also formed.

porphyrin plane is 0.29 Å; (2) the two independent pyrrole rings make angles of 16.6 and 11.3° with this plane; and (3) while *meso*-phenyl rings in 5,10,15,20-tetraphenylporphyrinato complexes typically make angles near 90° with the porphyrin plane, the two independent *meso*-phenyl rings in the present compound make angles of 43.1 and 43.6° with the porphyrin mean plane. As a rough measure of the height and width of the cavity note that the distance from the center of the four N atoms to the center of the C(34)–C(34a) bond is 9.28 Å while the distance between atoms C(27) and C(27a) is 10.46 Å.

Epoxidations. Initially we believed that a bulky phenoxide ligand could be employed to block the unhindered face of these chiral manganese porphyrins during asymmetric epoxidation reactions. This is a strategy similar to that used successfully with the picnic-basket porphyrin catalysts in shape-selective epoxidation.¹¹ However, using bulky phenoxide ligands with the manganese threitol-strapped porphyrins gave very low enantioselectivities. Curiously, we found that relatively high stereoselectivities are obtained with these catalysts when no blocking ligands are used in catalytic epoxidation reactions. An epoxidation reaction performed in the absence of added blocking ligands will herein be referred to as a “blank” reaction. This phenomenon of high stereoselectivity during a blank reaction is illustrated in the catalytic epoxidation of various olefins with iodosylbenzene by **3b** (Table 2). Up to 59% ee is achieved in the epoxidation of *cis*- β -methylstyrene (entry 10), making this system comparable to the most effective asymmetric metalloporphyrin catalysts.

Inoue observed modest enantioselectivities (16–18%) in blank reactions catalyzed by manganese(III) derivatives of mono-faced chiral porphyrins and higher selectivities (up to 54%) with reactions conducted in the presence of various imidazole ligands.⁶¹ Since nitrogenous ligands like imidazole and pyridine bind strongly to manganese(III) porphyrin derivatives ($K \approx 1000$),²⁰ several groups have proposed that the active oxidant in these systems is a manganese–oxo species with a *trans*-axial nitrogen heterocycle.²¹ The steric clash between the chiral substituents and the imidazole ligand presumably favors coordination of the imidazole to the unsubstituted face of the metalloporphyrin, thereby forcing the formation of the active

(20) Collman, J. P.; Brauman, J. I.; Fitzgerald, J. P.; Hampton, P. D.; Naruta, Y.; Michida, T. *Bull. Chem. Soc. Jpn.* **1988**, *61*, 47–57.

Table 3. % ee from the Asymmetric Epoxidation of 4-Chlorostyrene and *cis*- β -Methylstyrene Catalyzed by Manganese Threitol-Strapped Porphyrins: Effect of Added Pyridine or 4-*tert*-Butylpyridine^a

catalyst	4-chlorostyrene			<i>cis</i> - β -methylstyrene		
	blank	pyridine	4- <i>tert</i> -butylpyridine	blank	pyridine	4- <i>tert</i> -butylpyridine
3a	43	29	39	43	24	38
3b	44	27	28	59	24	37
3c	17	0	9	2	1	4 ^b
7	36	17	34	22	5	23
8	55	34	50	58		
9	58	32	58	59	34	61

^a Reactions were generally run for 1 h with 1.0 μ mol of catalyst, 100 μ mol of iodosylbenzene, 250 μ mol of pyridine or 4-*tert*-butylpyridine (if applicable), 20 μ L of nonane or dodecane, and 1.00 mmol of olefin in 2 mL of dry CH₂Cl₂ under nitrogen. Enantiomeric excesses were determined by Cyclodex-B chiral capillary column or by ¹H NMR spectroscopy in the presence of Eu(hfc)₃. Absolute configurations of the major product isomers are *R*(+) for 4-chlorostyrene and 1*R*,2*S*(-) for *cis*- β -methylstyrene (except where noted) and were assigned by comparison of polarimetry measurements with the literature. ^b The absolute configuration of the major isomer is 1*S*,2*R*(+).

oxo species and the subsequent oxygen-atom transfer to occur within the chiral cavity.

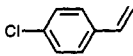
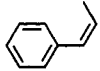
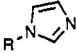
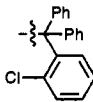
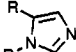

Table 3 presents the results from a similar study with the threitol-strapped manganese porphyrin system, in which 4-chlorostyrene and *cis*- β -methylstyrene served as model substrates for mono- and *cis*-disubstituted olefins. These olefins were epoxidized with iodosylbenzene catalyzed by the various manganese threitol-strapped porphyrins under three sets of conditions: blank reactions (reactions with no added ligands), reactions run in the presence of pyridine, and reactions run in the presence of 4-*tert*-butylpyridine. In each case, pyridine addition lowers the enantioselectivities compared to those obtained in the corresponding blank reactions. However, higher enantioselectivities are generally obtained with 4-*tert*-butylpyridine relative to those obtained with pyridine.

This study of the effect of added nitrogen ligands was expanded using **9** (the most effective catalyst in Table 3) to include imidazole derivatives (Table 4). As with pyridine ligands, low enantioselectivities are observed when small imidazole ligands are added to the epoxidation reactions (entries 1 and 2). However, employing larger imidazole derivatives dramatically increases the enantiomeric excess obtained. Thus, with chlortrimazole (entry 3), a commercially available 1-tritylimidazole derivative, and 1,5-diphenyl- and 1,5-dicyclohexylimidazole (entries 4 and 5, respectively), up to 70% ee is obtained in the epoxidation of 4-chlorostyrene and up to 77% ee in the epoxidation of *cis*- β -methylstyrene. These are the highest stereoselectivities reported in the epoxidation of those olefins with chiral metalloporphyrin catalysts.

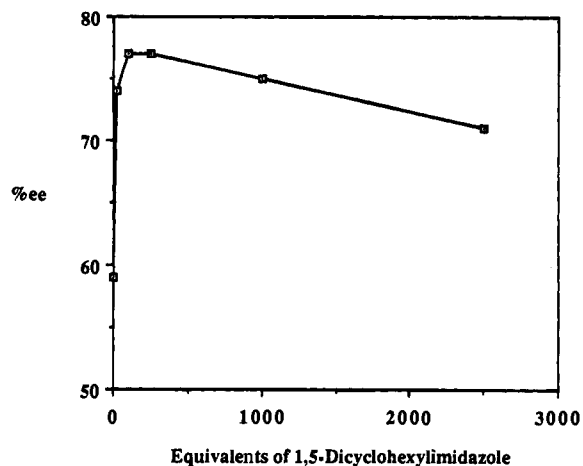
The concentration of 1,5-dicyclohexylimidazole required to optimize the enantioselectivities of the *cis*- β -methylstyrene

(21) (a) Guilmet, E.; Meunier, B. *Tetrahedron Lett.* **1982**, 2449–2452. (b) Meunier, B.; Guilmet, E.; De Carvalho, M.-E.; Poilblanc, R. *J. Am. Chem. Soc.* **1984**, *106*, 6668–6676. (c) Meunier, B.; Guilmet, E.; De Carvalho, M.-E.; Bortolini, O.; Momenau, M. *Inorg. Chem.* **1988**, *106*, 161–164. (d) Collman, J. P.; Kodadek, T.; Raybuck, S. A.; Meunier, B. *Proc. Natl. Aca. Sci. U.S.A.* **1983**, *80*, 7039–7041. (e) Collman, J. P.; Brauman, J. I.; Meunier, B.; Raybuck, S. A.; Kodadek, T. *Proc. Natl. Aca. Sci. U.S.A.* **1984**, *81*, 3245–3248. (f) Traylor, T. G.; Lee, W. A.; Stynes, D. V. *J. Am. Chem. Soc.* **1984**, *106*, 755–764. (g) Mansuy, D.; Battioni, P.; Renaud, J. P. *J. Chem. Soc., Chem. Commun.* **1984**, 1255–1257. (h) Battioni, P.; Renaud, J. P.; Bartoli, J. F.; Reina-Artiles, M.; Fort, M.; Mansuy, D. *J. Am. Chem. Soc.* **1988**, *110*, 8462–8470. (i) Yuan, L.-C.; Bruce, T. C. *J. Am. Chem. Soc.* **1986**, *108*, 1643–1650. (j) Lee, R. W.; Nakagaki, P. C.; Bruce, T. C. *J. Am. Chem. Soc.* **1989**, *111*, 1368–1372. (k) Groves, J. T.; Stern, M. K. *J. Am. Chem. Soc.* **1988**, *110*, 8628–8638.

Table 4. % ee from the Asymmetric Epoxidation of 4-Chlorostyrene and *cis*- β -Methylstyrene Catalyzed by the Out/Out Isomer, **9**: Effect of Added Imidazole Ligands^a

entry	ligand	ee, %	
			
1		0	6 ^b
2	R = CH ₃	1	5 ^b
3		69	76
4		66	74
5		70	77

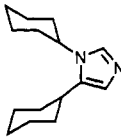
^a Reactions were generally run for 1 h with 1.0 μ mol of **9**, 100 μ mol of iodosylbenzene, 250 μ mol of the imidazole ligand, 20 μ L of nonane or dodecane, and 1.00 mmol of olefin in 2 mL of dry CH₂Cl₂ under nitrogen. Enantiomeric excesses were determined by Cyclodex-B chiral capillary column. The absolute configurations of the major product isomers are *R*(+) for 4-chlorostyrene and 1*R*,2*S*(-) for *cis*- β -methylstyrene (except where noted), and were assigned by comparison of polarimetry measurements with literature values. ^b The absolute configuration of the major product is 1*S*,2*R*(+).

**Figure 4.** The dependence of %ee on the concentration of 1,5-dicyclohexylimidazole used in the epoxidation of *cis*- β -methyl styrene by iodosylbenzene with **9**.

epoxidation catalyzed by **9** was also examined (Figure 4). The highest stereoselectivities are obtained when 100–250 equiv of the imidazole ligand (based on the catalyst) are added to the epoxidation reactions. It is estimated that greater than 99+% of the manganese porphyrin catalyst has a bound 1,5-dicyclohexylimidazole ligand in this optimum concentration range (see calculation in Appendix 1). At lower concentrations, the catalyst having only a chloride ligand might be able to compete with the imidazole-bound catalyst, resulting in lower enantiomeric excesses. At higher imidazole concentrations, the decrease in the stereoselectivity could arise from the formation of the bis-imidazole ligated species which might labilize the unhindered imidazole, allowing a small amount of the oxidation to proceed from the unsubstituted face of the catalyst.

Competition experiments were performed (Table 5) to estimate how much of the reaction is occurring on the unsubstituted face of **9**. In these experiments, equimolar mixtures of

Table 5. Competitive Epoxidation of 4-Chlorostyrene and *cis*-Stilbene: Quantification of Leakage in the Out/Out Isomer, **9**^a

entry	catalyst	ligand	ee, %		
			ee, %	yield, ^b %	yield, ^{b,c} %
1	Mn(TPP)Cl	None	0	32	68
2	9	None	66	74	26
3	9		70	90	10

^a Reactions were generally run for 1 h with 1.0 μ mol of catalyst, 100 μ mol of iodosylbenzene, 250 μ mol of 1,5-dicyclohexylimidazole (if present), 20 μ L of nonane, 0.5 mmol of 4-chlorostyrene, and 0.5 mmol of *cis*-stilbene in 2 mL of dry CH₂Cl₂ under nitrogen. Enantiomeric excesses were determined by Cyclodex-B chiral capillary column. The absolute configurations of the major product isomers are *R*(+) for 4-chlorostyrene oxide and were assigned by comparison of polarimetry measurements with literature values. ^b Yields are based upon consumption of iodosylbenzene and were determined by GC analysis. ^c Combined yields of *cis*- and *trans*-stilbene oxides.

4-chlorostyrene and *cis*-stilbene were epoxidized in the presence of a porphyrin catalyst. Three different catalyst systems were used in this study: Mn(TPP)Cl, **9**, and **9** in the presence of 1,5-dicyclohexylimidazole. The yields of both epoxides and enantiomeric excesses of the 4-chlorostyrene oxide are reported.

Table 6 presents the asymmetric epoxidation results obtained with several different olefins, with iodosylbenzene catalyzed by **9** in the presence of 1,5-dicyclohexylimidazole. The highest enantioselectivities achieved with other asymmetric catalysts are also provided for comparison. This threitol-strapped porphyrin catalyst yields up to 88% ee in the epoxidation of 1,2-dihydronaphthalene. While *cis*-disubstituted olefins are currently the most effective substrates, the catalyst also effectively epoxidizes mono-substituted olefin derivatives, giving up to 79% ee in the epoxidation of *o*-methylstyrene. Lower selectivities are obtained with *trans*-disubstituted olefins. The other enantiomer of **9** based on (*R,R*)-1,4-ditosylthreitol was also prepared and gives results similar to those presented in Table 6, affording epoxides with the opposite stereochemistry.

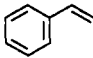
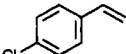
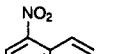
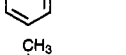
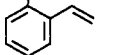
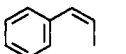
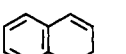
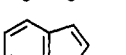
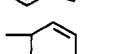
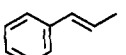
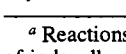
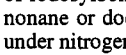
A limitation of this **9**/1,5-dicyclohexylimidazole catalyst system is that the enantiomeric excesses decrease at higher turnover numbers. This is illustrated in the asymmetric epoxidation of *cis*- β -methylstyrene (Figure 5). While the enantioselectivity is relatively constant at 77–78% up to 100 turnovers, it steadily declines to 57% at approximately 1000 turnovers. This decreased enantioselectivity is independent of the rate at which the iodosylbenzene is added to the reaction. This behavior is in contrast to that of chiral metallosalen epoxidation catalysts whose low catalytic turnovers are the result of a complete loss of catalytic activity.^{5d}

Another limitation of this porphyrin system is that oxidants other than iodosylbenzene give poorer results with these catalysts. Table 7 presents data from the epoxidation of 1,2-dihydronaphthalene and *cis*- β -methylstyrene with **9**/1,5-dicyclohexylimidazole and various oxidants that are commonly used in porphyrin-catalyzed epoxidation reactions. In general, these oxidants provide lower stereoselectivities and lower yields than are obtained with iodosylbenzene.

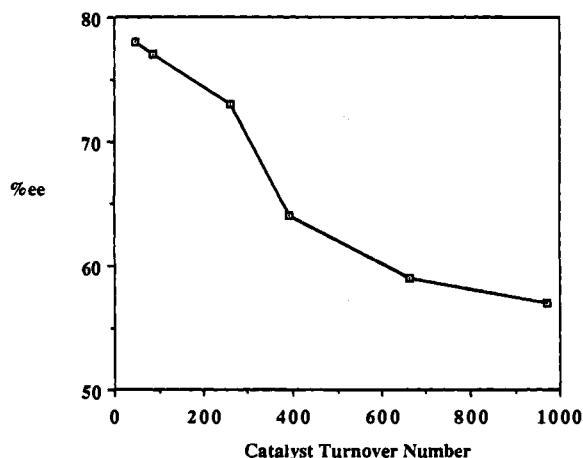
Discussion

The high enantioselectivities obtained in the blank reactions (reactions catalyzed by manganese(III) chloride porphyrins with

Table 6. Asymmetric Epoxidation of Olefins Catalyzed by the Out/Out Isomer, **9** with Added 1,5-Dicyclohexylimidazole^a

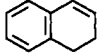
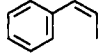
substrate	reaction temp, °C	yield, ^b %	ee, ^c %	configuration ^d	best reported ee, ^e %
	25	86	69	R(+)	57 ^f
	25	83	70	R(+)	51 ^g
	25	46	74	(-) ^h	89 ⁱ
	25	65 ^j	79	(-) ^h	16 ^g
	25	89	78	1R,2S(-)	92 ^k
	0	76	80		
	25	85	84		
	0	67	87	1R,2R(+)	92 ^l
	-10	26	88		
	25	84	74		70 ^l
	25	77	35	(-) ^h	
	25	81	21	1S,2S(-)	56 ^l

^a Reactions were generally run for 1 h with 1.0 μ mol of **9**, 100 μ mol of iodosylbenzene, 250 μ mol of 1,5-dicyclohexylimidazole, 20 μ L of nonane or dodecane, and 1.00 mmol of olefin in 2 mL of dry CH₂Cl₂ under nitrogen. ^b Yields are based upon consumption of iodosylbenzene and were determined by GC analysis. ^c Determined by Cyclodex-B chiral capillary column or by ¹H NMR spectroscopy in the presence of Eu(hfc)₃. ^d Assigned by comparison of polarimetry measurements with literature. ^e These values correspond to the highest ee's previously for non-enzymatic catalysts. ^f From ref 5a. ^g From ref 6a. ^h The absolute configuration was not determined. ⁱ From ref 6f. ^j A 30% yield of aldehyde was also detected. ^k From ref 5f. ^l From ref 5k.

**Figure 5.** The dependence of %ee on the catalyst turnover number for the epoxidation of *cis*- β -methylstyrene by iodosylbenzene with the Out/Out Isomer, **9** in the presence of 1,5-dicyclohexylimidazole.

no ligand other than the axial chloride) deserve comment. The reactive species is believed to be a high-valent metal-oxo intermediate,⁸ and control experiments indicate that negligible oxidation occurs in the absence of the metalloporphyrin catalysts. Three possible explanations could account for the behavior observed in these blank reactions: (1) epoxidation occurs exclusively on the unhindered face of the porphyrin, (2) the reaction occurs exclusively on the face of the porphyrin bearing the chiral straps, or (3) reaction occurs on both porphyrin faces to varying degrees. If pathway 1 is valid, then the

Table 7. Asymmetric Epoxidation of 4-Chlorostyrene and 1,2-Dihydronaphthalene Catalyzed by the Out/Out Isomer, **9** with Added 1,5-Dicyclohexylimidazole: Effect of Different Oxidants^a

oxidant				
	ee, %	yield, ^b %	ee, %	yield, ^b %
PhIO	84	85	78	89
H ₂ O ₂ ^c	68	29		
NaOCl ^d	12	75		
LiOCl ^e	12	55		
^t BuOOH			0	41
2,4,6-Me ₃ PhIO			7 ^f	80

^a Reactions were generally run for 1 h with 1.0 μ mol of **9**, 100 μ mol of oxidant, 250 μ mol of 1,5-dicyclohexylimidazole, 20 μ L of nonane or dodecane, and 1.00 mmol of olefin in 2 mL of dry CH₂Cl₂ under nitrogen. Enantiomeric excesses were determined by Cyclodex-B chiral capillary column or by ¹H NMR spectroscopy in the presence of Eu(hfc)₃. The absolute configurations of the major product isomers are 1R,2S(+) for 1,2-dihydronaphthalene and 1R,2S(-) for *cis*- β -methylstyrene (except where noted) and were assigned by comparison of polarimetry measurements with literature values. ^b Yields are based upon oxidant and were determined by GC analysis. ^c Reaction run as described in footnote a except in 1 mL of a 1:1 mixture of CH₂Cl₂:CH₃CN using 176 μ mol of H₂O₂ (30% in H₂O). ^d Reaction run as described in footnote a except using commercial bleach as the oxidant with 100 μ mol of 1,5-dicyclohexylimidazole and 25 μ mol Me₂(PhCH₂)NC₁₄H₂₉Cl in 2.5 mL of a 2:3 mixture of CH₂Cl₂:H₂O. ^e Reaction run as described in footnote d using a standardized stock solution of LiOCl as the oxidant. ^f The absolute configuration of the major product is 1S,2R(+).

unhindered face of the porphyrin ligand must be highly asymmetric. While the chiral straps of these mono-faced porphyrins might induce an asymmetric environment on the opposing face of the porphyrin, this effect should be modest. The high degree of asymmetric induction reported in Table 2 argues against the first hypothesis. Second, if the epoxidation occurs exclusively on the strapped face of the porphyrin, the optical yields reported in these blank reactions should be the maximum obtainable for these catalysts. However, higher enantioselectivities are achieved when bulky nitrogenous ligands are added to the epoxidation reactions (Tables 4 and 6) making hypothesis 2 unlikely. The third rationale is the most consistent with our experimental data. In the absence of added nitrogenous ligands, the catalyst appears to be in an initial conformational isomer that fortuitously favors the oxidation within the chiral straps. It seems reasonable that this is due to the chloride ligand being bound preferentially to the unstrapped face of the metalloporphyrin. This regioisomer appears to be very stable since addition of excess chloride ligand does not lower the observed optical yields.²² This result implies that halide exchange occurs with retention on the same face of the porphyrin. The blank catalyst, having a manganese(III) chloride group, may also have an intrinsically different reactivity compared with catalysts that have coordinated, neutral ligands such as imidazoles or pyridines. The neutral ligands should replace the chloride anion affording a manganese center with a higher formal positive charge. Such a change could increase the reactivity of the manganese-oxo center. The lower enantiomeric excesses observed at higher catalyst turnover numbers (Figure 5) are thought to result from either scrambling of the initial catalyst conformation in the course of the epoxidation reactions or degradation of the chiral superstructure of the catalyst. Either of these would produce a less-stereoselective catalyst system.

The results obtained from the addition of pyridine and imidazole ligands to these reactions (Tables 3 and 4) are

(22) The addition of 100 equiv of [Bz(Et)₃N]Cl to the epoxidation of 4-chlorostyrene with **9** gives 64% ee of the corresponding epoxide. This is slightly higher than the 58% ee obtained in the comparable reaction without added chloride (Table 3).

consistent with the model proposed above. For small ligands such as pyridine (Table 3) and imidazole (Table 4), the interaction between the chiral threitol substituents and the ligand is apparently negligible, allowing the ligand to bind to either side of the catalyst. This also permits oxo transfer to proceed from either face of the porphyrin, resulting in low enantiomeric excesses during catalysis. Larger ligands such as 4-*tert*-butylpyridine (Table 3) or substituted imidazoles (Table 4) are sterically inhibited from binding between the chiral straps of the porphyrin; thus they should preferentially bind to the unsubstituted face of the catalyst. This would force epoxidation to occur within the chiral pocket of the porphyrin catalyst and result in stereoselectivity increases relative to those obtained with pyridine or imidazole. As expected, the steric interaction with the larger ligands appears to be most pronounced with the bridged-porphyrin catalysts, 7–9 (Table 3).

The results from the competition experiments reported in Table 5 can be used to approximate how much epoxidation is occurring on the unhindered face of **9** (i.e. the leakage of the catalyst). In this study, the product ratio of 4-chlorostyrene oxide to stilbene oxides (32:68) obtained with Mn(TPP)Cl (Entry 1) is used to approximate the relative reactivity of the corresponding olefins on the unsubstituted face of the catalyst, **9**. Since *cis*-stilbene is sterically bulky, we assume that the stilbene oxide products are formed solely from reactions on the open face of the threitol-strapped catalyst. Thus, the 26% yield of stilbene oxides obtained with **9** (Entry 2) implies that 12% ($26\% \times 32/68$) of the total 4-chlorostyrene oxide is produced on the unsubstituted face of the catalyst during a blank reaction. Similarly, 5% ($10\% \times 32/68$) of the total 4-chlorostyrene oxide produced when 1,5-dicyclohexylimidazole is added to the reaction mixture also arises from oxidation on the unsubstituted face of the catalyst (Entry 3). Thus the estimated leakage to the unhindered face of **9** is 38% ($26\% + 12\%$) when no ligand is added and 15% ($10\% + 5\%$) when 1,5-dicyclohexylimidazole is added to the catalyst system.

Alternatively, these results can be used to determine the efficiency of the asymmetric induction of the chiral cavity. Since oxidation on the open face presumably has no chiral induction, the enantiomeric excess of the material produced inside the cavity must be greater than the overall observed enantiomeric excess. The observed enantiomeric excess can therefore be corrected for leakage and the enantiomeric excess of reaction within the cavity can be determined. For example, if 12% of the 4-chlorostyrene oxides formed during a blank reaction are produced via leakage on the unhindered face of the catalyst (calculations above, from Entry 2), these 12% should be present as a racemic mixture (i.e. 6% *R* and 6% *S*). The remaining 62% of the 4-chlorostyrene oxide produced in this reaction is formed inside the chiral cavity and, in the case of perfect asymmetric induction, would be a single enantiomer (i.e. 62% *R*). The observed overall enantiomeric excess of 66% (Entry 2) leads to a calculated ee inside the cavity of **9** of 78% ($R_{\text{outside}} = S_{\text{outside}} = 6\%$, $R_{\text{inside}} + S_{\text{inside}} = 62\%$, see calculation in Appendix 2). Similarly, in the case where 1,5-dicyclohexylimidazole is added to the reaction mixture (Entry 3), 5% of the 4-chlorostyrene oxide is produced through leakage to the unhindered face of the catalyst and the remaining 85% is formed inside the chiral cavity. The observed enantiomeric excess under these conditions is 70%; the ee inside the cavity is therefore calculated to be 74% ($R_{\text{outside}} = S_{\text{outside}} = 2.5\%$, $R_{\text{inside}} + S_{\text{inside}} = 85\%$, see calculation in Appendix 2).²³

(23) When the competitive epoxidation of *cis*-stilbene and 4-chlorostyrene catalyzed by **9** in the presence of 1,5-dicyclohexylimidazole is repeated using H₂O₂ as the oxidant, the calculated enantiomeric excess inside the basket is also 74% ($R_{\text{outside}} = S_{\text{outside}} = 2.5\%$, $R_{\text{inside}} + S_{\text{inside}} = 84\%$, ee_{obs} = 70%). See calculation in Appendix 2.

These competition results indicate that a more effective means of blocking the unhindered face of **9** is necessary if this catalyst is to be of commercial interest. This may comprise the use of more effective blocking ligands or the addition of sacrificial substrates that preferentially react with metal–oxo groups formed on the unhindered face of the catalyst. The effectiveness of this latter approach is illustrated in the epoxidation of 4-chlorostyrene with **9** in which the enantioselectivity increases from 58% (Table 3) to 66% (Table 5) when *cis*-stilbene is added to the reaction. However, these results also clearly indicate that the cavity of **9** does not afford perfect asymmetric induction; further modifications to the cavity itself may prove to be a more effective means of improving this catalyst system.

Two explanations could account for the lower selectivities at higher turnover numbers illustrated in Figure 5. First, the catalyst could be undergoing partial degradation, possibly as the result of intramolecular processes. While UV–vis data indicate that the porphyrin ring is intact, mass spectrometry of the catalyst recovered from an oxidation reaction reveals the presence of some higher molecular weight species, consistent with the introduction of oxygen atoms to the recovered porphyrin catalyst. These data are compatible with partial oxidation of the chiral superstructure. The second explanation is that the reaction produces a byproduct that functions as a ligand to the manganese porphyrin in subsequent catalytic cycles. Since the high enantiomeric excesses of this system depend on the effective blocking of the unhindered face of the manganese porphyrin catalyst by a bulky imidazole ligand, the formation of a smaller ligand that could bind to either face of the catalyst could lower the observed enantiomeric excess. While the identify of such a byproduct is unknown, it could result from the partial oxidative decomposition of 1,5-dicyclohexylimidazole, since similar imidazole ligands are known to be effective substrates in oxidation reactions catalyzed by manganese porphyrins.²⁴ Also, the presence of small ligands in these epoxidation reactions can have a dramatic effect on the stereoselectivity of the reaction. For example, the addition of 5 equiv of 1-methylimidazole to the 1,2-dihydronaphthalene oxidation at 25 °C presented in Table 6 lowers the observed optical yield from 84% ee to 49% ee, despite the presence of a 50-fold excess of 1,5-dicyclohexylimidazole. Thus, the formation of a small amount of a byproduct that functions as a ligand to the manganese porphyrin could lead to large decreases in enantiomeric excesses.

There are also at least two explanations that may explain the lower selectivities that are obtained with different oxidants (Table 7). The first is that these other oxidants are modifying the catalyst in some way, either by reacting with the catalyst superstructure or by promoting the scrambling of the axial ligand to form an active oxidizing species on the unhindered face of the metalloporphyrin. The second possibility is that the active oxidant is not a discrete high-valent metal–oxo species but is rather a metalloporphyrin–oxidant complex. The stereoselectivity obtained with such complexes would then be dependent upon the structures of both the oxidant and the catalyst as well as the interaction between the two.

These experimental results also indicate the stereochemical-defining interactions are not between the bridge over the catalyst and the olefin substituents. Figure 3 shows a stereoview of the In/In isomer **4**, and schematic representations of such a structure are shown in Figure 6. Also shown in Figure 6 are what we believe are reasonable schematic representations of an Out/Out isomer, although no crystal structure of such an isomer is available. These top views reveal that the straps of the In/In

(24) Collman, J. P.; Brauman, J. I.; Hampton, P. D.; Tanaka, H.; Bohle, D. S.; Hembre, R. T. *J. Am. Chem. Soc.* **1990**, *112*, 7980–7984.

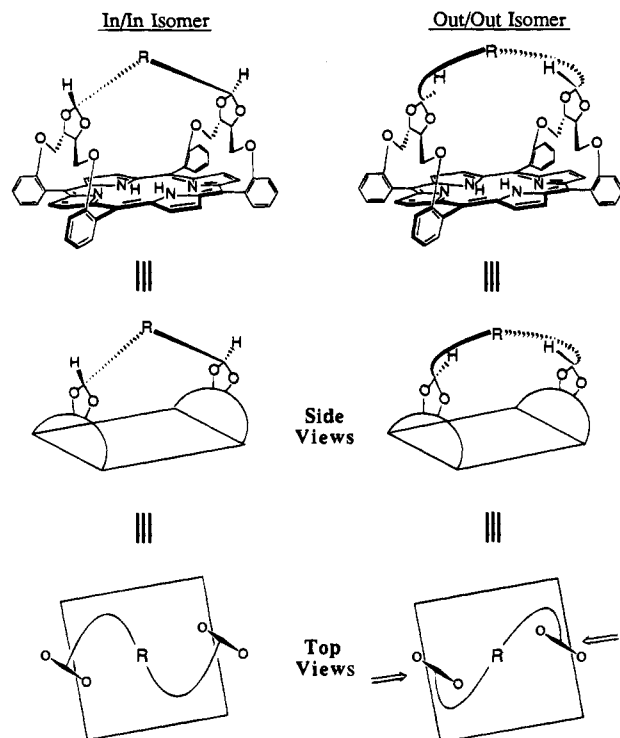


Figure 6. Drawings of the In/In and Out/Out isomers of the bridged, threitol-strapped porphyrins and schematic representations of the side views and top views of each system. The bridge of the Out/Out isomer pulls the threitol rings closer to the center of the macrocycle.

and Out/Out porphyrins have different "chiral senses." If the major interaction of an approaching prochiral olefin is between the bridges of the strapped catalyst and the olefin substituents, then a *cis*-disubstituted olefin (or a monosubstituted olefin when $R_1 = H$) would approach the reactive site as shown in Figure 7a in the case of the In/In isomer and as shown in Figure 7b in the case of the Out/Out isomer. Each of these approaches minimizes the interaction between the strap and the smaller olefin substituent R_1 . However, these two different approaches would lead to the production of epoxides with different stereochemistries, which is inconsistent with the results presented in Table 3 for these two catalyst systems.

The experimental results can be explained if the major interactions are between the olefin substituents and the inner oxygen atom of the dioxolane unit of the threitol straps. Such a model predicts that the approach depicted in Figure 7c is the dominant pathway in the case of the In/In isomer and that depicted in Figure 7b is the dominant pathway in the case of the Out/Out isomer. These approaches avoid a steric clash between the inner threitol oxygen atoms and the substituent R_1 on the olefin (that occurs in the approaches shown in Figures 7a and 7d) and predict the preferred formation of the observed major epoxide enantiomers. These results are consistent with the side-on approach of the olefin to the metal-oxo as originally proposed by Groves,²⁵ and elaborated on by other authors.²⁶

This model also explains why the Out/Out isomer is a more effective catalyst than the In/In isomer. If it is assumed that the threitol straps are fixed, then the bridge of the Out/Out isomer has to span a greater distance than it would in the In/In

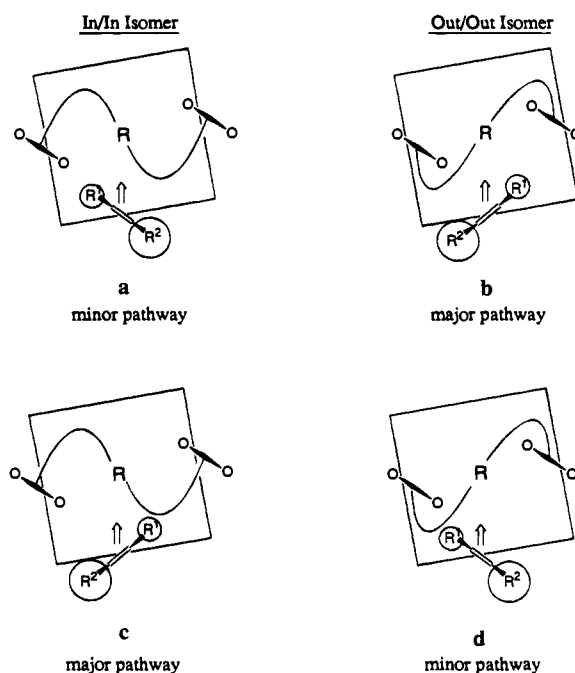


Figure 7. The different approaches of a *cis*-disubstituted olefin (or a monosubstituted olefin when $R^1 = H$) to both the In/In and Out/Out isomers of the bridged threitol-strapped porphyrins. The major pathways for each system (c and b, respectively) result from the steric interactions between the olefin substituents and the inner oxygen atom of the threitol straps.

isomer. This results from the bridge of the Out/Out isomer pointing out, away from the center of the macrocycle, and having to wrap back around to make a similar connection on the other side of the catalyst. However, since both of these straps have the same connectivity, the catalyst must compensate for the different stereochemistry by allowing the threitol straps to be pulled closer to the center of the macrocycle in the Out/Out isomer (Figure 6, top view of the Out/Out isomer). This makes the minor pathway of the Out/Out isomer (Figure 7d) less favorable than the minor pathway of the In/In isomer (Figure 7a). Thus, higher enantioselectivities are obtained with the Out/Out isomer.

Conclusions

This paper has described the facile syntheses of several single-faced, threitol-strapped porphyrins. The chiral environments of these porphyrins are readily modified by employing different acetal or ketal protecting groups in the 2,3-diol positions of the threitol units, allowing optimization of the catalyst design.

Manganese(III) chloride derivatives of these porphyrin systems were found to be effective asymmetric epoxidation catalysts. When no ligands are added to block the unhindered face of the porphyrin, moderate enantioselectivities at low turnover numbers result. An examination of the effect of added nitrogen ligands on the asymmetric catalysis reveals that lower optical yields are obtained with each catalyst when small ligands like pyridine or imidazole are added to the epoxidation reactions. This presumably results from the ability of these smaller ligands to bind to both faces of the metalloporphyrin, allowing the oxo-transfer to occur primarily from the unhindered face of the catalyst. Higher stereoselectivities are obtained with larger imidazole and pyridine ligands, presumably because their size disfavors their binding within the chiral cavity; thus they preferentially bind to the open face of the catalyst, forcing the oxidation to occur between the chiral straps.

The bridged, threitol-strapped systems exhibit the most pronounced effect from the addition of these bulky nitrogen

(25) (a) Groves, J. T.; Nemo, T. E. *J. Am. Chem. Soc.* **1983**, *105*, 5786–5791. (b) Groves, J. T.; Han, Y.; Van Engen, D. *J. Chem. Soc., Chem. Commun.* **1990**, 436–437.

(26) (a) Traylor, T. G.; Miksztal, A. R. *J. Am. Chem. Soc.* **1989**, *111*, 7443–7448. (b) Ostović, D.; Bruce, T. C. *J. Am. Chem. Soc.* **1989**, *111*, 6511–6517. (c) Ostović, D.; Bruce, T. C. *J. Am. Chem. Soc.* **1988**, *110*, 6906–6908. (d) He, G.-X.; Mei, H.-Y.; Bruce, T. C. *J. Am. Chem. Soc.* **1991**, *113*, 5644–5650.

ligands. Up to 88% ee is obtained with *cis*-disubstituted olefins and up to 79% ee is obtained with monosubstituted olefins in asymmetric epoxidation reactions catalyzed by the Out/Out porphyrin complex (**9**) in the presence of 1,5-dicyclohexylimidazole. This 9/1,5-dicyclohexylimidazole system is among the most effective chiral metalloporphyrin catalysts yet reported for the asymmetric epoxidation of unfunctionalized olefins and is the most effective catalyst for the asymmetric epoxidation of simple, monosubstituted olefins. Apparently the function of the bridge is to pull the threitol rings closer to the center of the macrocycle.

Experimental Section

Materials. All solvents were purchased from Fisher Scientific Co., were of reagent grade quality, and were used without further purification (except where noted). All reagents were purchased from Aldrich Chemical Co., Inc., and were used as received (except where noted). Dry methylene chloride was distilled from P₂O₅ under a nitrogen atmosphere. Dry DMF and dry *o*-dichlorobenzene were anhydrous grade and were purchased from Aldrich Chemical Co., Inc. *cis*- β -Methylstyrene was purchased from K&K Laboratories. 2-Methylstyrene and 4-nitrostyrene were purchased from Pfaltz & Bauer. Chlorotrimazole was purchased from Sigma Scientific. Anhydrous manganese(II) bromide was purchased from Alfa. Thionyl chloride was distilled from triphenyl phosphite under nitrogen. Deuterated solvents were purchased from Cambridge Isotope Laboratories and were stored over activated 4Å molecular sieves. Silica gel for flash chromatography was Type 7741, manufactured by E. M. Science and distributed by VWR Inc. All olefins used in the epoxidation studies were filtered (neat or dissolved in pentane) through a plug of alumina immediately prior to their use.

The following compounds were prepared by literature procedures: (*S,S*)-threitol 1,4-di-*p*-tosylate (**13**),²⁷ 5,10,15,20-tetrakis(2-hydroxyphenyl)porphyrin (**10**),¹⁴ (*S,S*)-*trans*-4,5-bis[(*p*-tosyloxy)methyl]-2,2-diphenyl-1,3-dioxolane (**11b**),¹⁶ 1,5-diphenylimidazole,²⁸ and 2-nitrostyrene.²⁹

Physical Methods. NMR spectra were obtained on a Varian 400 MHz spectrometer. UV-vis spectra were taken on a Hewlett Packard 8452A Diode Array spectrometer. Elemental analyses were obtained from Chemical Analytic Services, Berkeley, CA, or from Midwest Microlab, Indianapolis, IN. Mass spectra were recorded at the Mass Spectrometry Resource, School of Pharmacy, University of California at San Francisco, San Francisco, CA. Gas chromatography was performed on a Hewlett Packard 5890A gas chromatograph with the use of either a SE-54 capillary column (0.32 × 15 m) to determine the reaction yields or a chiral Cyclodex-B capillary column (0.25 × 30 m) to determine the enantiomeric excesses. Both columns were obtained from J & W Scientific Co.

9,9-Dichloroxanthene Synthesis (14c). A 50 mL round-bottomed flask equipped with a condenser, a nitrogen inlet, and a stirring bar is charged with xanthone (3.00 g, 15 mmol), thionyl chloride (30 mL), and DMF (3 drops). The mixture is heated under nitrogen at reflux (4 h) and then cooled to room temperature. The excess thionyl chloride is removed under vacuum. The sealed flask is then taken into a nitrogen-filled drybox where the product is collected (3.77 g, 100%).

¹H NMR (CDCl₃) δ 8.13 (dd, *J* = 8.0, 1.6 Hz, 2H), 7.39 (m, 2H), 7.26 (m, 2H), 7.12 (dd, *J* = 8.4, 1.2 Hz, 2H).

1,2-Bis(3-formylphenoxy)ethane (15). A dry 100 mL, round-bottomed flask equipped with a nitrogen inlet and a stirring bar is charged with 3-hydroxybenzaldehyde (4.89 g, 40 mmol), 1,2-dibromoethane (1.60 mL, 18.6 mol), potassium carbonate (10.0 g, 0.72 mmol), and DMF (300 mL). The mixture is heated at 60 °C under nitrogen (3 days) while 1,2-dibromoethane aliquots (0.5 mL, 6 mmol) are added to the solution at 12 h intervals. The solution is then cooled and is poured into water (500 mL) and stirred (1 h). The precipitate that forms is collected by filtration. This solid is dissolved in CH₂Cl₂ (300 mL) and washed with 5% aqueous NaOH (2 × 1 L) and then

water (100 mL). The final organic layer is dried over MgSO₄, filtered, and condensed to give the desired product (1.21 g, 22%).

¹H NMR (CDCl₃) δ 9.91 (s, 2H), 7.46–7.51 (m, 6H), 7.23–7.27 (m, 2H), 4.43 (s, 4H). MS: *m/e* 270 for C₁₆H₁₄O₄. Anal. Calcd for C₁₆H₁₄O₄: C, 71.10; H, 5.22. Found: C, 71.02; H, 5.23.

Xanthone-Protected Ditosylated Strap Synthesis (11c).¹⁶ In an inert atmosphere drybox, a 50 mL, 2-necked, pear-shaped flask is charged with **14c** (2.51 g, 10 mmol) and the flask is equipped with a Vigreux condenser, a nitrogen inlet, and a magnetic stirring bar. The apparatus is stoppered and brought out of the drybox and charged with (*S,S*)-threitol 1,4-di-*p*-tosylate (4.30 g, 10 mmol) and dry *o*-dichlorobenzene (30 mL) under nitrogen. A slow stream of nitrogen is bubbled through the mixture and the solution is stirred at reflux (12 h). The mixture is then cooled to room temperature and the solvent is removed under reduced pressure. The black solid that remains is dissolved in CH₂Cl₂ (10 mL) and filtered through a plug of silica gel with additional CH₂Cl₂ (100 mL) as the eluent. The filtrate is condensed to a solid and the material is recrystallized from benzene/heptane (3.65 g, 60%).

¹H NMR (CDCl₃) δ 7.74 (d, *J* = 7.9 Hz, 4H), 7.59 (d, *J* = 7.9 Hz, 2H), 7.36–7.42 (m, 2H), 7.28 (d, *J* = 8.0 Hz, 4H), 7.21 (d, *J* = 8.3 Hz, 2H), 7.13–7.17 (m, 2H), 4.54 (bs, 2H), 4.33 (bs, 4H), 2.42 (s, 6H). MS: *m/e* 608 for C₃₁H₂₈O₉S₂. Anal. Calcd for C₃₁H₂₈O₉S₂: C, 61.17; H, 4.64; S, 10.53. Found: C, 60.87; H, 4.55; S, 10.09.

Tetratosylated Strap Synthesis (12). A 100 mL, round-bottomed flask equipped with a magnetic stirring bar is charged with the appropriate dialdehyde (1.00 g, 3.70 mmol), (*S,S*)-threitol 1,4-di-*p*-tosylate (6.37 mmol, 15 mmol), *p*-toluenesulfonic acid (10 mg), and toluene (60 mL). A Dean-Stark trap fitted with a water-cooled condenser and a nitrogen inlet are attached to the flask. The mixture is stirred under nitrogen at reflux (12 h). The mixture is cooled to room temperature, pyridine (*ca.* 1 mL) is added to the solution, and the material is condensed to a solid. The product is purified by flash chromatography on silica gel with 2% ethyl acetate/CH₂Cl₂ as the eluent. The first major band is collected and condensed to give the desired product (3.37 g, 83%).

¹H NMR (CDCl₃) δ 7.81 (d, *J* = 8.2 Hz, 4H), 7.75 (d, *J* = 8.2 Hz, 4H), 7.36 (d, 8.2 Hz, 4H), 7.31 (d, *J* = 8.2 Hz, 4H), 7.23–7.27 (m, 2H), 6.91–6.97 (m, 6H), 5.78 (s, 2H), 4.32 (s, 4H), 4.13–4.21 (m, 12H), 2.45 (s, 6H), 2.42 (s, 6H). MS: *m/e* 1095 (M + H)⁺ for C₅₂H₅₄O₁₈S₄. Anal. Calcd for C₅₂H₅₄O₁₈S₄: C, 57.03; H, 4.97; S, 11.71. Found: C, 57.14; H, 5.00; S, 11.53.

Bis-Strapped Porphyrins. General Procedure (1a–c, 2a–c). A 250 mL, 3-necked, round-bottomed flask equipped with a nitrogen inlet and a magnetic stirring bar is charged with the appropriate dithreitol derivative (2.5 mmol), **10** (679 mg, 1.0 mmol), and dry DMF (200 mL). The mixture is heated under nitrogen to 100 °C, K₂CO₃ (1.69 g, 12 mmol) is added, and stirring is continued (16 h). The mixture is cooled to room temperature, diluted with CH₂Cl₂ (300 mL), and washed with water (300 mL). The final organic layer is dried over Na₂SO₄, filtered, and condensed to a purple solid. The material is purified as described below.

1a and **2a** were flash chromatographed on silica gel using CH₂Cl₂ as the eluent. The first band is the Up/Down isomer (**1a**) followed by a major band that is the Up/Up isomer (**2a**). Each of these bands is collected and condensed, and the solids are recrystallized from CH₂Cl₂/MeOH (**1a**: 39 mg, 4.2%. **2a**: 307 mg, 33%).

1a. ¹H NMR (CDCl₃) δ 9.27 (s, 2H), 9.18 (s, 2H), 8.69 (dd, *J* = 7.4, 1.6 Hz, 2H), 8.43 (d, *J* = 4.6 Hz, 2H), 8.37 (dd, *J* = 7.3, 1.6 Hz, 2H), 8.34 (d, *J* = 4.6 Hz, 2H), 7.69–7.79 (m, 4H), 7.58–7.64 (m, 2H), 7.47–7.52 (m, 2H), 7.40–7.43 (m, 2H), 7.21–7.24 (m, 2H), 4.67–4.72 (m, 2H), 4.05 (t, *J* = 8.7 Hz, 2H), 3.85–3.89 (m, 4H), 3.47 (d, *J* = 9.0 Hz, 2H), 1.79–1.86 (m, 2H), 0.60 (s, 6H), –1.07 (s, 6H), –2.28 (s, 2H, D₂O exchangeable). UV-vis (CH₂Cl₂): λ 407 (sh), 426 (Soret), 490 (sh), 522, 558, 604, 664 nm. MS: *m/e* 931 (M + H)⁺ for C₅₈H₅₀N₄O₈. Anal. Calcd for C₅₈H₅₀N₄O₈: C, 74.82; H, 5.41; N, 6.02. Found: C, 74.47; H, 5.31; N, 5.95.

2a. ¹H NMR (CDCl₃) δ 8.91 (d, *J* = 4.8 Hz, 2H), 8.87 (d, *J* = 4.8 Hz, 2H), 8.62 (dd, *J* = 7.4, 1.6 Hz, 2H), 8.38 (d, *J* = 4.5 Hz, 2H), 8.29 (d, *J* = 4.6 Hz, 2H), 8.24 (dd, *J* = 7.4, 1.6 Hz, 2H), 7.72–7.78 (m, 4H), 7.56–7.60 (m, 2H), 7.41–7.47 (m, 4H), 7.27 (d, *J* = 7.3 Hz, 2H), 4.68–4.70 (m, 2H), 4.14 (t, *J* = 8.8 Hz, 2H), 3.90–3.96 (m, 4H), 3.55 (d, *J* = 9.1 Hz, 2H), 2.20 (m, 2H), 0.64 (s, 6H), –0.93 (s, 6H),

(27) Dumont, W.; Poulin, J.-C.; Dang, T.-P.; Kagan, H. B. *J. Am. Chem. Soc.* **1973**, *95*, 8295–8299.

(28) van Leusen, A. M.; Wildeman, J.; Oldenziel, O. H. *J. Org. Chem.* **1977**, *42*, 1153–1159.

(29) Wiley, R. H.; Smith, N. R. *J. Am. Chem. Soc.* **1950**, *72*, 5198–5199.

–2.12 (s, 2H, D₂O exchangeable). UV–vis (CH₂Cl₂): λ 408 (sh), 426 (Soret), 490 (sh), 522, 566, 606, 666 nm. MS: *m/e* 931 (M + H)⁺ for C₅₈H₅₀N₄O₈. Anal. Calcd for C₅₈H₅₀N₄O₈: C, 74.82; H, 5.41; N, 6.02. Found: C, 74.64; H, 5.39; N, 6.07.

1b and **2b** were flash chromatographed on silica gel using CH₂Cl₂ as the eluent. The first band is the Up/Down isomer (**1b**) followed by a major band that is the Up/Up isomer (**2b**). Each of these bands is collected and condensed, and the solids are recrystallized from CH₂Cl₂/MeOH (**1b**: 132 mg, 11%. **2b**: 485 mg, 41%).

1b. ¹H NMR (CDCl₃) δ 9.33 (s, 2H), 9.16 (s, 2H), 8.68 (dd, *J* = 7.4, 1.7 Hz, 2H), 8.50 (d, *J* = 7.3 Hz, 2H), 8.41 (d, *J* = 4.4 Hz, 2H), 8.32 (d, *J* = 4.4 Hz, 2H), 7.72–7.80 (m, 4H), 7.62 (t, *J* = 7.5 Hz, 2H), 7.56 (t, *J* = 7.6 Hz, 2H), 7.41 (d, *J* = 8.1 Hz, 2H), 7.25 (d, *J* = 8.1 Hz, 2H), 6.87–6.98 (m, 6H), 6.73 (d, *J* = 7.9 Hz, 4H), 5.12 (d, *J* = 8.1 Hz, 4H), 4.97 (t, *J* = 7.3 Hz, 2H), 4.81 (d, *J* = 10.6 Hz, 2H), 4.14–4.21 (m, 6H), 3.91–3.96 (m, 4H), 3.72 (d, *J* = 9.0 Hz, 2H), 2.05 (m, 2H), –2.33 (s, 1H, D₂O exchangeable), –2.54 (s, 1H, D₂O exchangeable). UV–vis (CH₂Cl₂): λ 407 (sh), 428 (Soret), 490 (sh), 522, 558, 606, 664 nm. MS: *m/e* 1179 (M + H)⁺ for C₇₈H₅₈N₄O₈. Anal. Calcd for C₇₈H₅₈N₄O₈: C, 79.44; H, 4.96; N, 4.75. Found: C, 79.39; H, 4.89; N, 4.86.

2b. ¹H NMR (CDCl₃) δ 9.03 (d, 4.9 Hz, 2H), 8.80 (d, *J* = 4.5 Hz, 2H), 8.63 (dd, *J* = 7.4, 1.6 Hz, 2H), 8.35 (d, *J* = 4.5 Hz, 2H), 8.29 (d, *J* = 4.5 Hz, 2H), 8.23 (dd, *J* = 7.4, 1.6 Hz, 2H), 7.69–7.77 (m, 4H), 7.57–7.60 (m, 2H), 7.42 (t, *J* = 7.4 Hz, 2H), 7.36 (d, *J* = 8.3 Hz, 2H), 7.25 (d, *J* = 8.0 Hz, 2H), 7.27 (t, *J* = 7.3 Hz, 2H), 6.78–6.81 (m, 4H), 6.57 (d, *J* = 7.3 Hz, 4H), 5.43 (t, *J* = 7.4 Hz, 2H), 5.07 (d, *J* = 7.3 Hz, 4H), 4.69–4.72 (m, 6H), 4.10 (t, *J* = 8.9 Hz, 2H), 3.92–3.97 (m, 4H), 3.80 (d, *J* = 8.4 Hz, 2H), 2.50 (m, 2H), –2.16 (s, 2H, D₂O exchangeable). UV–vis (CH₂Cl₂): λ 409 (sh), 428 (Soret), 491 (sh), 524, 558, 608, 666 nm. MS: *m/e* 1179 (M + H)⁺ for C₇₈H₅₈N₄O₈. Anal. Calcd for C₇₈H₅₈N₄O₈: C, 79.44; H, 4.96; N, 4.75. Found: C, 79.75; H, 4.86; N, 4.79.

1c and **2c** were flash chromatographed on silica gel using 20% hexanes/CH₂Cl₂ as the eluent. The first band is the Up/Down isomer (**1c**) followed by a major band that is the Up/Up isomer (**2c**). Each of these bands is collected and condensed, and the solids are recrystallized from CH₂Cl₂/MeOH (**1c**: 206 mg, 17%. **2c**: 288 mg, 24%).

1c. ¹H NMR (CDCl₃) δ 9.39 (s, 2H), 9.22 (s, 2H), 8.65 (d, *J* = 6.9 Hz, 2H), 8.54 (d, *J* = 4.7 Hz, 2H), 8.50 (d, *J* = 6.4 Hz, 2H), 8.38 (d, *J* = 4.7 Hz, 2H), 7.80–7.83 (m, 2H), 7.71–7.74 (m, 2H), 7.57–7.62 (m, 4H), 7.45 (d, *J* = 8.2 Hz, 2H), 7.28 (d, *J* = 8.3 Hz, 2H), 7.21 (d, *J* = 7.8 Hz, 2H), 7.06–7.10 (m, 2H), 6.91–6.95 (m, 2H), 6.71 (d, *J* = 8.0 Hz, 2H), 6.14 (d, *J* = 8.3 Hz, 2H), 5.88–5.92 (m, 2H), 4.94 (d, *J* = 10.3 Hz, 2H), 4.28–4.36 (m, 4H), 4.10–4.13 (m, 4H), 4.03 (d, *J* = 9.0 Hz, 2H), 2.39–2.44 (m, 4H), –1.82 (s, 1H, D₂O exchangeable), –2.35 (s, 1H, D₂O exchangeable). UV–vis (CH₂Cl₂): λ 407 (sh), 428 (Soret), 490 (sh), 522, 556, 604, 664 nm. MS: *m/e* 1207 (M + H)⁺ for C₇₈H₅₄N₄O₁₀. Anal. Calcd for C₇₈H₅₄N₄O₁₀: C, 77.60, H, 4.51; N, 4.64. Found: C, 77.40; H, 4.50; N, 4.66.

2c. ¹H NMR (CDCl₃) δ 9.04 (d, *J* = 4.8 Hz, 2H), 8.93 (d, *J* = 4.8 Hz, 2H), 8.65 (dd, *J* = 7.3, 1.6 Hz, 2H), 8.47 (d, *J* = 4.7 Hz, 2H), 8.37 (d, *J* = 4.6 Hz, 2H), 8.33 (dd, *J* = 7.4, 1.7 Hz, 2H), 7.81 (dt, *J* = 1.6, 7.8 Hz, 2H), 7.68 (dt, *J* = 1.7, 7.9 Hz, 2H), 7.59–7.63 (m, 2H), 7.40–7.46 (m, 4H), 7.23–7.28 (m, 4H), 7.10–7.14 (m, 2H), 6.93–6.97 (m, 2H), 6.77 (dd, *J* = 8.2, 1.0 Hz, 2H), 5.27–5.31 (m, 2H), 5.06 (dd, *J* = 8.4, 1.0 Hz, 2H), 4.74 (d, *J* = 10.9 Hz, 2H), 4.45 (t, *J* = 8.8 Hz, 2H), 4.19 (d, *J* = 8.4 Hz, 2H), 3.99 (d, *J* = 8.3 Hz, 2H), 3.92 (d, *J* = 9.6 Hz, 2H), 3.92 (d, *J* = 9.6 Hz, 2H), 3.56 (dd, *J* = 7.8, 1.1 Hz, 2H), 2.58 (m, 2H), 1.49 (m, 2H), –1.94 (s, 2H, D₂O exchangeable). UV–vis (CH₂Cl₂): λ 408 (sh), 428 (Soret), 490 (sh), 522, 556, 606, 666 nm. MS: *m/e* 1207 (M + H)⁺ for C₇₈H₅₄N₄O₁₀. Anal. Calcd for C₇₈H₅₄N₄O₁₀: C, 77.60, H, 4.51; N, 4.64. Found: C, 77.36; H, 4.48; N, 4.55.

Bridged Porphyrins (4–6). A dry, 500 mL, 3-necked, round-bottomed flask equipped with a nitrogen inlet and a magnetic stirring bar is charged with **12** (1.18 g, 1.1 mmol), **10** (611 mg, 0.90 mmol), and dry DMF (200 mL). The mixture is heated under nitrogen to 100 °C K₂CO₃ (1.49 g, 11 mmol) is added, and stirring is continued (16 h). The mixture is cooled to room temperature, diluted with CH₂Cl₂ (300 mL), and washed with water (350 mL). The final organic layer is dried over Na₂SO₄, filtered, and condensed to a purple solid. This material is purified by flash chromatography with 2% ethyl acetate/CH₂Cl₂ as

the eluent. The first purple band is the Out/Out isomer (**c**), followed by a purple band that is the In/Out isomer (**b**). The eluent is changed to 5% ethyl acetate/CH₂Cl₂ and a third band is collected, which is the In/In isomer (**a**). Each of these bands is collected and condensed, and the solids are recrystallized from CH₂Cl₂/MeOH (**4**: 45 mg, 4.6%. **5**: 223 mg, 23%. **6a**: 151 mg, 16%).

4. ¹H NMR (CD₂Cl₂) δ 8.87 (dd, *J* = 7.6, 4.7 Hz, 4H), 8.54 (dd, *J* = 7.4, 1.6 Hz, 2H), 8.42 (d, *J* = 4.5 Hz, 2H), 8.33 (dd, *J* = 7.5, 1.7 Hz, 2H), 8.28 (d, *J* = 4.6 Hz, 2H), 7.75–7.83 (m, 4H), 7.60 (t, *J* = 7.5 Hz, 2H), 7.48–7.52 (m, 4H), 7.42 (d, *J* = 8.2 Hz, 2H), 6.48–6.52 (m, 2H), 6.34–6.40 (m, 4H), 6.12 (s, 2H), 5.39 (s, 2H), 4.37–4.42 (m, 2H), 4.19–4.25 (m, 4H), 4.00 (d, *J* = 9.2 Hz, 2H), 3.87–3.89 (m, 2H), 3.61 (s, 4H), 2.51 (m, 2H), –2.20 (s, 2H, D₂O exchangeable). UV–vis (CH₂Cl₂): λ 409 (sh), 428 (Soret), 493 (sh), 524, 560, 608, 670 nm. MS: *m/e* 1085 (M + H)⁺ for C₆₈H₅₂N₄O₁₀.

5. ¹H NMR (CDCl₃) δ 8.88–8.90 (m, 3H), 8.84 (d, *J* = 4.7, 1H), 8.50–8.55 (m, 2H), 8.43 (d, *J* = 4.5 Hz, 1H), 8.41 (d, *J* = 4.6 Hz, 1H), 8.36–8.39 (m, 2H), 8.27–8.32 (m, 2H), 7.71–7.79 (m, 4H), 7.41–7.59 (m, 7H), 7.29 (d, *J* = 7.9 Hz, 1H), 6.93 (t, *J* = 7.9 Hz, 1H), 6.75 (d, *J* = 7.5 Hz, 1H), 6.54–6.57 (m, 1H), 6.54–6.57 (m, 1H), 6.35–6.39 (m, 1H), 6.26 (s, 1H), 6.19 (d, *J* = 7.4 Hz, 1H), 5.86 (s, 1H), 5.46 (s, 1H), 5.01 (d, *J* = 9.8 Hz, 1H), 4.46–4.51 (m, 1H), 4.38 (s, 1H), 4.31–4.36 (m, 2H), 4.10–4.23 (m, 4H), 3.92 (dd, *J* = 10.3, 4.5 Hz, 1H), 3.81 (d, *J* = 8.8 Hz, 1H), 3.62–3.70 (m, 4H), 2.93 (m, 1H), 2.70 (m, 1H), –2.11 (s, 2H, D₂O exchangeable). UV–vis (CH₂Cl₂): λ 409 (sh), 428 (Soret), 492 (sh), 524, 560, 608, 670 nm. MS: *m/e* = 1085 (M + H)⁺ for C₆₈H₅₂N₄O₁₀H₂O. Anal. Calcd for C₆₈H₅₂N₄O₁₀H₂O: C, 74.03; H, 4.93; N, 5.08. Found: C, 73.69; H, 4.84; N, 4.91.

6. ¹H NMR (CDCl₃) δ 8.98 (d, *J* = 4.6 Hz, 2H), 8.93 (d, *J* = 4.8 Hz, 2H), 8.62 (d, *J* = 7.3 Hz, 2H), 8.45 (d, *J* = 4.6 Hz, 2H), 8.36 (d, *J* = 4.4 Hz, 2H), 8.27 (dd, *J* = 7.4, 1.8 Hz, 2H), 7.75–7.81 (m, 4H), 7.58–7.62 (m, 4H), 7.50 (t, *J* = 7.4 Hz, 2H), 7.34 (d, 8.3 Hz, 2H), 6.95 (t, *J* = 8.0 Hz, 2H), 6.77 (d, *J* = 7.4 Hz, 2H), 6.57 (dd, *J* = 8.0, 1.7 Hz, 2H), 5.98 (s, 2H), 5.08 (d, *J* = 10.3 Hz, 2H), 4.55 (s, 2H), 4.42 (t, *J* = 8.8 Hz, 2H), 4.24 (d, *J* = 10.6 Hz, 2H), 4.18 (d, *J* = 9.5 Hz, 2H), 3.90 (d, *J* = 8.6 Hz, 2H), 3.72–3.78 (m, 4H), 2.80 (m, 2H), –2.08 (s, 2H, D₂O exchangeable). UV–vis (CH₂Cl₂): λ 410 (sh), 430 (Soret), 492 (sh), 526, 562, 608, 670 nm. MS: *m/e* 1085 (M + H)⁺ for C₆₈H₅₂N₄O₁₀H₂O. Anal. Calcd for C₆₈H₅₂N₄O₁₀H₂O: C, 74.03; H, 4.93; N, 5.08. Found: C, 73.66; H, 4.84; N, 4.91.

Manganese Insertions (3a–c, 7–9). General Procedure. A 50 mL, round-bottomed flask equipped with a magnetic stirring bar is charged with the chiral porphyrin (30 mg), dry DMF (30 mL), 2,6-leutidine (3 drops), and anhydrous MnBr₂ (120 mg). The mixture is heated at 100 °C (24–96 h) in air until the Soret band of the free base porphyrin is replaced by that of the manganese porphyrin. The mixture is then cooled and washed with a brine solution (2 × 50 mL). The final organic layer is dried over NaCl, filtered, and condensed to a solid. This solid is dissolved in CH₂Cl₂ (5 mL) and filtered through a plug of silica gel using CH₂Cl₂/ethyl ether (1/1) (50 mL) as the eluent. The filtrate is again condensed and the product is precipitated from CH₂Cl₂/heptane (90–100%).

3a. UV–vis (CH₂Cl₂): λ 384, 408 (sh), 486 (Soret), 544, 596, 632 nm. MS: *m/e* 983 (M + 1 – Cl) for C₅₈H₄₈ClMnN₄O₈.

3b. UV–vis (CH₂Cl₂): λ 386, 410 (sh), 488 (Soret), 540, 596, 634 nm. MS: *m/e* 1231 (M + 1 – Cl) for C₇₈H₅₆ClMnN₄O₈.

3c. UV–vis (CH₂Cl₂): λ 386, 406 (sh), 486 (Soret), 538, 596, 632 nm. MS: *m/e* 1276 (M + 1 – Cl) for C₇₈H₅₂ClMnN₄O₈.

7. UV–vis (CH₂Cl₂): λ 386, 410 (sh), 486 (Soret), 540, 596, 632 nm. MS: *m/e* 1137 (M + 1 – Cl) for C₆₈H₅₀ClMnN₄O₁₀.

8. UV–vis (CH₂Cl₂): λ 386, 410 (sh), 490 (Soret), 540, 600, 636 nm. MS: *m/e* 1137 (M + 1 – Cl) for C₆₈H₅₀ClMnN₄O₁₀.

9. UV–vis (CH₂Cl₂): λ 386, 410 (sh), 488 (Soret), 544, 600, 636 nm. MS: *m/e* 1137 (M + 1 – Cl) for C₆₈H₅₀ClMnN₄O₁₀. Anal. Calcd for C₆₈H₅₀ClMnN₄O₁₀·3H₂O: C, 66.53; H, 4.60; N, 4.56, Cl, 2.89. Found: C, 66.58; H, 4.19; N, 4.54, Cl, 3.17.

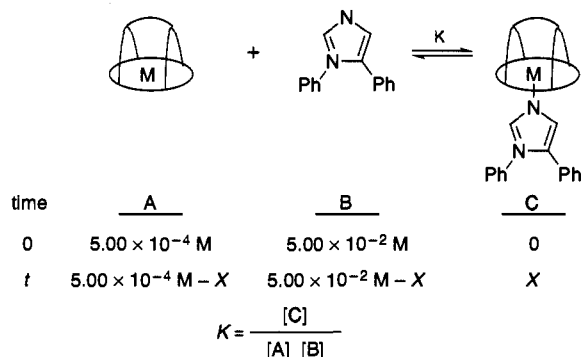
Typical Asymmetric Epoxidation Procedure with PhIO: A dry, 20 mL, side-arm flask is purged with nitrogen and charged with the chiral porphyrin catalyst (1.0 μ mol), dry CH₂Cl₂ (2 mL), axial ligand (250 μ mol, if applicable), olefin (1.00 mmol), and an internal standard (20 μ L). Iodosylbenzene (22 mg, 100 μ mol) is added and the mixture is rapidly stirred (1 h). Aliquots (5 μ L) are removed from the reaction mixture at appropriate intervals and are quenched with a 2% triph-

enylphosphine solution in CH_2Cl_2 (50 μL). These aliquots are used to monitor the formation of the product. The mixture is filtered through a plug of glass wool and condensed to an oil. The product is purified by chromatography on silica gel with the use of pentane to remove the remaining olefin and 20% ethyl ether/pentane to elute the product. The enantiomeric excess is determined by ^1H NMR spectroscopy in the presence of a chiral shift reagent or by injection onto a chiral GC column. Polarimetric measurement of the oxidized product dissolved in CH_2Cl_2 is used to determine the optical rotation of the major enantiomer.

Acknowledgment. We thank the National Institutes of Health (Grant 5R37 GM-17880-22 to J.P.C.; Grant HL-13157 to J.A.I.) for funding this work. We also thank Drs. Erich Uffelman, Scott Bohle, and Peter Erk for helpful discussions. C.K.-Y. gratefully acknowledges an N.S.F. Predoctoral Fellowship and X.Z. gratefully acknowledges the Franklin Veatch Fellowship from the Department of Chemistry, Stanford. Mass spectroscopic analyses were conducted at the regional N.I.H. Mass Spectroscopy Facility, San Francisco, CA.

Appendix 1

When a 100-fold excess of axial ligand is used:



With $K = 1000$ (ref 20):

$$1000 = \frac{X}{(5.00 \times 10^{-4} - X)(5.00 \times 10^{-2} - X)} \Rightarrow X = 4.90 \times 10^{-4}$$

Therefore, the percent of bound catalyst at a 100-fold excess of imidazole is

$$\frac{4.90 \times 10^{-4}}{5.00 \times 10^{-4}}(100\%) = 98\%$$

Similarly, 100% of the catalyst is in the bound state when a 250-fold excess of the imidazole ligand is used.

Appendix 2

To correct the observed enantiomeric excess for the leakage reaction:

$$ee_{\text{obs}} = \frac{R_{\text{total}} - S_{\text{total}}}{R_{\text{total}} + S_{\text{total}}} = \frac{(R_{\text{inside}} + R_{\text{outside}}) - (S_{\text{inside}} + S_{\text{outside}})}{(R_{\text{inside}} + R_{\text{outside}}) + (S_{\text{inside}} + S_{\text{outside}})} = \frac{R_{\text{inside}} + R_{\text{outside}} - S_{\text{inside}} - S_{\text{outside}}}{R_{\text{inside}} + R_{\text{outside}} + S_{\text{inside}} + S_{\text{outside}}}$$

Since $R_{\text{outside}} = S_{\text{outside}}$

$$ee_{\text{obs}} = \frac{R_{\text{inside}} - S_{\text{inside}}}{(R_{\text{inside}} + S_{\text{inside}}) + (R_{\text{outside}} + S_{\text{outside}})} = \frac{R_{\text{inside}} - S_{\text{inside}}}{(R_{\text{inside}} + S_{\text{inside}}) \left[1 + \frac{(R_{\text{outside}} + S_{\text{outside}})}{(R_{\text{inside}} + S_{\text{inside}})} \right]}$$

By rearrangement:

$$\frac{R_{\text{inside}} - S_{\text{inside}}}{R_{\text{inside}} + S_{\text{inside}}} = ee_{\text{obs}} \left[1 + \frac{(R_{\text{outside}} + S_{\text{outside}})}{(R_{\text{inside}} + S_{\text{inside}})} \right] = ee_{\text{inside}}$$

In the absence of added ligand:

$$R_{\text{outside}} = S_{\text{outside}} = 6, \quad R_{\text{inside}} + S_{\text{inside}} = 62, \quad ee_{\text{obs}} = 66$$

Therefore:

$$ee_{\text{inside}} = 66 \left(1 + \frac{12}{62} \right) = 79$$

In the presence of 1,5-dicyclohexylimidazole:

$$R_{\text{outside}} = S_{\text{outside}} = 2.5, \quad R_{\text{inside}} + S_{\text{inside}} = 85, \quad ee_{\text{obs}} = 70$$

Therefore:

$$ee_{\text{inside}} = 70 \left(1 + \frac{5}{85} \right) = 74$$

Supplementary Material Available: Tables of experimental crystallographic details, atomic coordinates and equivalent isotropic displacement parameters, bond lengths and angles, anisotropic displacement parameters, and hydrogen atom coordinates and isotropic displacement parameters (8 pages). Ordering information is given on any current masthead page. This material is contained in many libraries on microfiche, immediately follows this article in the microfilm version of the journal, and can be ordered from the ACS; see any current masthead page for ordering information.

JA942090B